Gastroenterology 2025;168:769–783

A Pangenotypic Hepatitis E Virus Replication Inhibitor With High Potency in a Rat Infection Model

Xin Zhang,[1] Mara Klöhn,[2] Sivi Ouwerkerk-Mahadevan,[3] Michelle Jagst,[2,4] Liesbeth Vereyken,[3] Peter Verboven,[3] Quinten Goovaerts,[5] Daniel Todt,[2,6] Tim H. M. Jonckers,[3] Lotte Coelmont,[1] Helen Fletcher,[7] Kalyan Das,[5] Kirandeep Samby,[7] Johan Neyts,[1] Eike Steinmann,[2,8] Anil Koul,[6,9] and Suzanne J. F. Kaptein[1]

[1]Department of Microbiology, Immunology and Transplantation, Rega Institute for Medical Research, Virology, Antiviral Drug & Vaccine Research Group, KU Leuven, Leuven, Belgium; [2]Department of Molecular and Medical Virology, Ruhr University Bochum, Bochum, Germany; [3]Janssen Research & Development, Janssen Pharmaceutica N.V., Beerse, Belgium; [4]Institute of Virology, University of Veterinary Medicine Hannover, Hannover, Germany; [5]Department of Microbiology, Immunology and Transplantation, Rega Institute for Medical Research, Molecular, Structural and Translational Virology Research Group, KU Leuven, Leuven, Belgium; [6]European Virus Bioinformatics Center (EVBC), Jena, Germany; [7]Janssen Global Public Health, Janssen Pharmaceutica, Beerse, Belgium; [8]German Centre for Infection Research (DZIF), External Partner Site, Bochum, Germany; and [9]Department of Infection Biology, London School of Hygiene & Tropical Medicine, London, United Kingdom

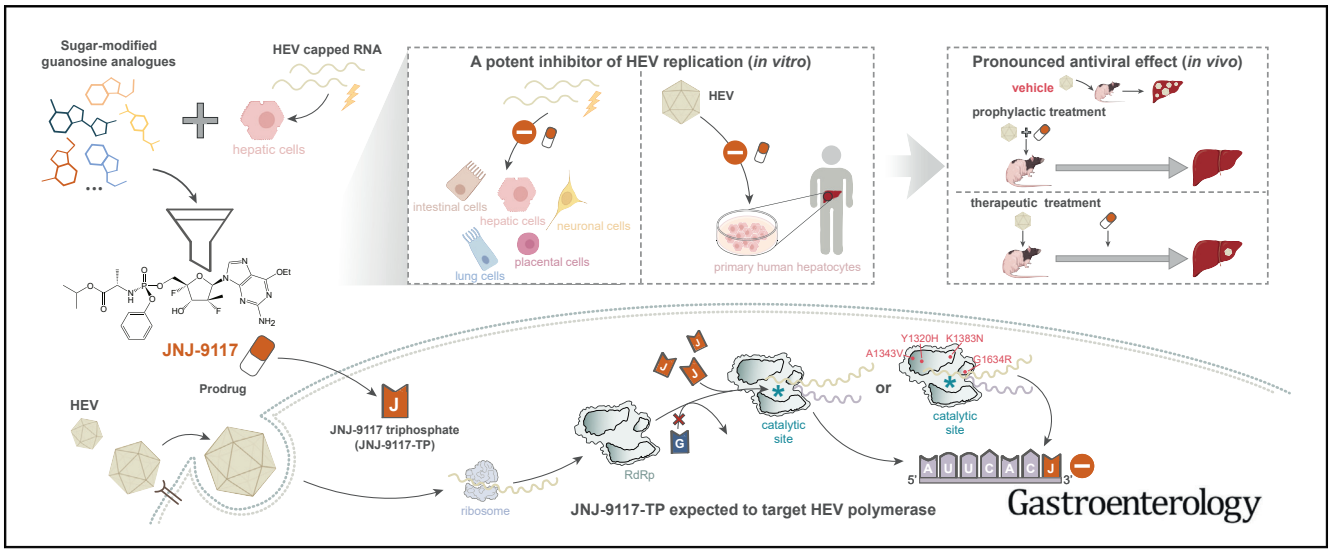

BACKGROUND & AIMS: Hepatitis E virus (HEV) constitutes a substantial public health burden with ∼20 million human infections annually, including 3.3 million symptomatic cases. Appropriate treatment options for, in particular, HEV-infected immunocompromised patients and pregnant women are lacking, underscoring the urgent need for potent and safe antiviral drugs. **METHODS:** HEV subgenomic replicon systems were used to screen a small library of preselected nucleoside analogues, originally developed in a hepatitis C virus (HCV) antiviral program. Antiviral activity of the selected hit on HEV infection was evaluated in a variety of cell culture systems, and the efficacy of the compound was assessed in the athymic nude rat HEV infection model. **RESULTS:** Compound JNJ-9117 exerts pangenotype antiviral activity against HEV in different cell types as well as in primary human hepatocytes. A high level of conservation is observed between 3 crucial motifs in the catalytic domain of the HCV and HEV polymerases. This suggests a mechanism of action that is identical to that of the molecule against HCV, whereby the 5′-triphosphate of JNJ-9117 acts as a chain terminator during viral RNA synthesis. JNJ-9117 has a favorable pharmacokinetic and safety profile in rats and results in a pronounced antiviral effect in a chronic rat HEV infection model, both in a prophylactic and therapeutic setting. The combination of JNJ-9117 and ribavirin (each at an intentionally selected suboptimal/inactive dose) was highly effective in infected rats in lowering the viral RNA load in liver and feces to (almost) undetectable levels. **CONCLUSIONS:** JNJ-9117 has a profile that holds promise for the treatment of life-threatening HEV infections in humans. Phase I studies with JNJ-9117 have been initiated in healthy human volunteers.

Keywords: Hepatitis E Virus (HEV); Antiviral Therapy; Nucleoside Analogue; Primary Human Hepatocytes; Rat HEV Infection Model.

The hepatitis E virus (HEV) is a leading cause of acute viral hepatitis.[1] Although most of the ∼20 million infections resolve spontaneously, ∼3.3 million symptomatic cases occur annually with symptoms such as fatigue, anorexia, abdominal pain, jaundice, and hepatomegaly, and an estimated 44,000 people die because of HEV infections.[2–4] In immunocompromised individuals, such as organ transplant recipients, HEV infections can lead to life-threatening chronic conditions.[5] Pregnant women, especially in their second or third trimester, are at high risk of acute liver failure and fetal loss, with a fatality rate of up to 25%.[6] HEV-1 and HEV-2, which are fecal-orally transmitted, infect only humans. These viruses are highly prevalent in low-income countries in Africa and Asia, where they pose a significant risk of acute liver failure and fetal loss.[7] HEV-3 and HEV-4 are zoonotic viruses and circulate mostly in developed countries, where contaminated food (undercooked/raw meat), blood transfusion, and organ transplantation represent the principal infection sources.[8] Some human infections have also been reported with the rat HEV (*Rocahepevirus ratti* species).[9]

There is one vaccine (HEV 239, Hecolin, Wantai BioPharm), which is based on HEV-1, that is only approved in China and Pakistan.[10] Treatment options are restricted to the off-label use of ribavirin, a drug with limited potency that is associated with serious adverse effects such as anemia and embryo-fetal toxicity. We demonstrated earlier that treatment failures with ribavirin in patients with chronic HEV infections can be linked to amino acid substitutions G1634R, Y1320H, and K1383N and an insertion in the hypervariable region.[11,12] The hepatitis C virus (HCV) polymerase inhibitor sofosbuvir was found to exert medium level in vitro activity against HEV[13] but is insufficiently potent to be used as monotherapy in patients with HEV infection.[14] We previously revealed that sofosbuvir treatment of HEV-infected patients can result in the emergence of drug-resistant variants (most notably A1343V).[15]

There is hence an urgent need for effective and safe drugs for the treatment of HEV infections. We here report that the nucleoside analogue JNJ-9117 has in vitro pangenotype anti-HEV activity and potent efficacy in a rat HEV infection model. This molecule was taken for single ascending dose studies in healthy human volunteers[16]; results will be reported in a separate publication.

WHAT YOU NEED TO KNOW

BACKGROUND AND CONTEXT

Hepatitis E virus causes high mortality in pregnant women and chronic infections in immunocompromised individuals, necessitating safer and more effective treatment than the currently available options that consist of ribavirin and pegylated interferon alfa.

NEW FINDINGS

The nucleoside analogue JNJ-9117 exerts potent pangenotype antiviral activity against hepatitis E virus across various cell types, including primary human hepatocytes. Additionally, JNJ-9117 possesses a favorable pharmacokinetic and safety profile and is highly effective in a chronic rat hepatitis E virus infection model.

LIMITATIONS

Efficacy and safety of JNJ-9117 in preclinical models of hepatitis E virus infection in pregnancy remain to be demonstrated.

CLINICAL RESEARCH RELEVANCE

JNJ-9117 may be an ideal molecule for further development for the treatment of hepatitis E virus infections. Also, patients with chronic hepatitis E that are refractory to ribavirin treatment may be expected to be responsive to treatment with JNJ-9117. The combination of JNJ-9117 with ribavirin may potentially be even more beneficial in managing life-threatening hepatitis E virus infections.

BASIC RESEARCH RELEVANCE

There is an unmet need for efficacious and safe antiviral drugs for the treatment of (chronic) hepatitis E virus infections. We demonstrate that a nucleoside analogue that targets (as its 5′-phosphorylated metabolite) the polymerase of the hepatitis C virus also exerts potent activity against hepatitis E virus, another but unrelated (+) single-stranded RNA virus. This work provides insight in how to target viral polymerases and achieving broader-spectrum antivirals.

Materials and Methods

Viruses

Plasmid constructs derived from HEV-3 full-length Kernow-C1 p6 (GenBank accession number JQ679013) and the variant Kernow-C1 p6 G1634R (containing the G1634R mutation in the viral polymerase) were described previously.[12] Construction of subgenomic Kernow-C1 p6/luc harboring a *Gaussia* luciferase gene downstream of the open reading frame 2 (ORF2) start codon was described earlier.[17] The HEV-1 reporter replicon Sar55/S17/luc was derived from the HEV strain Sar55/S17 (GenBank accession number AF444002).[18] The sequence of HEV-3 strain 83-2-27[19] is available in GenBank (accession number AB740232). Rat HEV LA-B350 (GenBank accession number KM516906) and plasmid pLA-B350/luc were described previously.[20] Single nucleotide variants of HEV-3 (Kernow-C1 p6/luc) were generated according to Gömer et al.[15]

Abbreviations used in this paper: **GTP, guanosine-5'-triphosphate; HCV, hepatitis C virus; HEV, hepatitis E virus; IC_{50}, 50% inhibitory concentration; IFN-α, interferon alfa; JNJ-9117-TP, 5′-triphosphate metabolite of JNJ-9117; LLOQ, lower limit of quantification; ORF2, open reading frame 2; RdRp, RNA-dependent RNA polymerase.**

Most current article

0016-5085
https://doi.org/10.1053/j.gastro.2024.10.043

Animal Experiments

Homozygous 4- to 5-week-old female athymic nude Hsd:RH-*Foxn1*^{rnu} rats (*Rattus norvegicus*, Envigo) were used in the animal experiments. Housing conditions and experimental procedures were approved by the KU Leuven Ethics Committee (P003/2021) and followed institutional guidelines approved by the Federation of European Laboratory Animal Science Associations. Rats were randomly assigned to different experimental groups and housed per 1 or 2 in individually ventilated cages (GR900, Sealsafe Plus, Tecniplast) at 21°C, 55% humidity, and 12:12 light:dark cycles. Rats were provided with food and water ad libitum, a cardboard house, and wooden gnawing blocks. During the animal experiments, rats were daily weighed and checked for clinical signs. At the end of the animal experiments, rats were humanely killed by intraperitoneal injection of pentobarbital (Dolethal, Vetoquinol UK Ltd).

Efficacy of JNJ-9117 in a prophylactic setting. Athymic nude rats were infected by intravenous injections of a 1% liver homogenate of rat HEV LA-B350 (200 μL; containing $\sim 1\times10^6$ viral RNA copies) in the tail vein.[20] To assess the prophylactic efficacy of JNJ-9117, athymic nude rats (n = 6 per group) were orally treated with vehicle (polyethylene glycol-400 and water [30% volume/volume]) or different doses (10, 35, or 100 mg/kg, per dose) of JNJ-9117. Vehicle and JNJ-9117 treatments, both twice-daily, started 12 hours before infection and continued until day 11 after infection. As a control, 1 group was treated with ribavirin (60 mg/kg, once daily by oral gavage), which started 2 hours before infection. From days 0 to 12 postinfection, feces were collected every 4 days. On day 12 postinfection, rats were euthanized, followed by the collection of blood (via cardiac puncture) and tissues (intestine, spleen, and liver). Samples were stored at −80°C until further use. The viral RNA load in the samples was quantified by reverse-transcription quantitative polymerase chain reaction.

Efficacy of JNJ-9117 in a therapeutic setting. The therapeutic potential of JNJ-9117 on an ongoing infection was assessed in delayed treatment studies. Rats (n = 10 for the vehicle group, n = 6 for the other groups) were treated with vehicle, JNJ-9117 (70 or 200 mg/kg/d, twice daily) or ribavirin (60 mg/kg/d, once daily). Treatment was initiated on day 5 or 10 after infection and continued for 11 days, hence ending on day 17 or day 22 postinfection, respectively.

On the day treatment was started (ie, day 5 or day 10 postinfection), 4 untreated rats (belonging to the vehicle groups) were euthanized for quantification of viral RNA in the collected samples (blood, intestine, spleen, and liver) at the time treatment was initiated. From days 0 to 17 postinfection (when treatment started on day 5 postinfection) or days 0 to 22 postinfection (when treatment started on day 10 postinfection), feces were collected every 4 to 5 days. At end point (ie, day 17 or day 22 postinfection), rats were euthanized and blood (via cardiac puncture), intestine, spleen, and liver were collected. Samples were stored at −80°C until further use (viral RNA quantification by reverse-transcription quantitative polymerase chain reaction).

Efficacy of the combination JNJ-9117 and ribavirin. As detailed earlier, rats were infected with rat HEV. They received treatment 2 hours before infection with vehicle, JNJ-9117 at 30 or 40 mg/kg/d (twice daily), ribavirin at 20 or 30 mg/kg (once daily), or a combined treatment consisting of JNJ-9117 (30 or 40 mg/kg, twice daily) and ribavirin (20 or 30 mg/kg, once daily). Treatment continued for 11 days, rats were monitored daily, and feces were collected every 4 days. Groups of rats were euthanized 12 days after infection to assess viral RNA in the collected samples (feces, blood, intestine, spleen, and liver). Samples were stored at −80°C until further processing.

In vivo resistance selection. Athymic nude rats (N = 3) were infected orally as described previously.[21] In brief, a diluted infectious liver homogenate (500 μL per rat, comprising $\sim 2\times10^7$ viral RNA copies) was orally administered on day 0 and day 2 postinfection. Infected rats received JNJ-9117 treatment (twice daily by oral gavage) starting on day 60 postinfection. Fecal samples were collected every 2 to 3 days, and doses of JNJ-9117 were adjusted when the viral RNA load in the feces had dropped to nearly undetectable levels. Treatment continued for 65 days for 1 rat and 70 days for the other 2 rats. Liver, intestine, and spleen samples were collected after euthanasia. Sequencing of the rat HEV RNA-dependent RNA polymerase (RdRp) domain from fecal samples (at the starting point and every 7 days from day 30 of treatment) and tissue samples (at the end point) was performed as previously described.

Additional methods are provided in the Supplementary Methods.

Results

JNJ-9117 Is a Potent Inhibitor of Hepatitis E Virus Replication

To identify molecules with antiviral activity against HEV, we assessed the effect of a selection of 19 sugar-modified guanosine analogues (with demonstrated in vitro antiviral activity against HCV[22]) on the replication of luciferase-encoding subgenomic replicons of HEV-3 (Kernow-C1 p6; for simplicity, we below refer to "HEV-3") and rat HEV (pLA-B350) in Huh7 cells (Figure 1*A* and *B* and Supplementary Table 1). The HCV polymerase inhibitor sofosbuvir[13] and ribavirin were included as positive controls. A few molecules within the series displayed nanomolar antiviral activity against both replicons (Figure 1*B*, blue dots represent compounds with a 50% inhibitory concentration (IC_{50}) of $\leq$100 nmol/L (Supplementary Table 1), of which JNJ-9117 (Figure 1*C*) inhibited the HEV-3 and rat HEV replicon replication with an IC_{50} of 21 nmol/L and 30 nmol/L, respectively (Figure 1*D* and *E*). Comparable antiviral potency was observed against a HEV-1 (Sar55/S17/luc) replicon (Figure 1*D* and *E*).

Compared with ribavirin and sofosbuvir, JNJ-9117 was respectively 300-fold and 30-fold more active against the HEV-3 replicon, 1500-fold and 40-fold more active against the rat HEV replicon, and 1800-fold and 100-fold more active against the HEV-1 replicon (Figure 1*D*–*G*). Furthermore, JNJ-9117 also potently inhibited the replication of the HEV-1 and HEV-3 subgenomic replicons in a range of other cell lines, both hepatic (IC_{50}: 10–150 nmol/L) and nonhepatic, including intestinal (IC_{50}: 150–300 nmol/L), neuronal (IC_{50}: 14–900 nmol/L), lung (IC_{50}: 85–145 nmol/L), and the

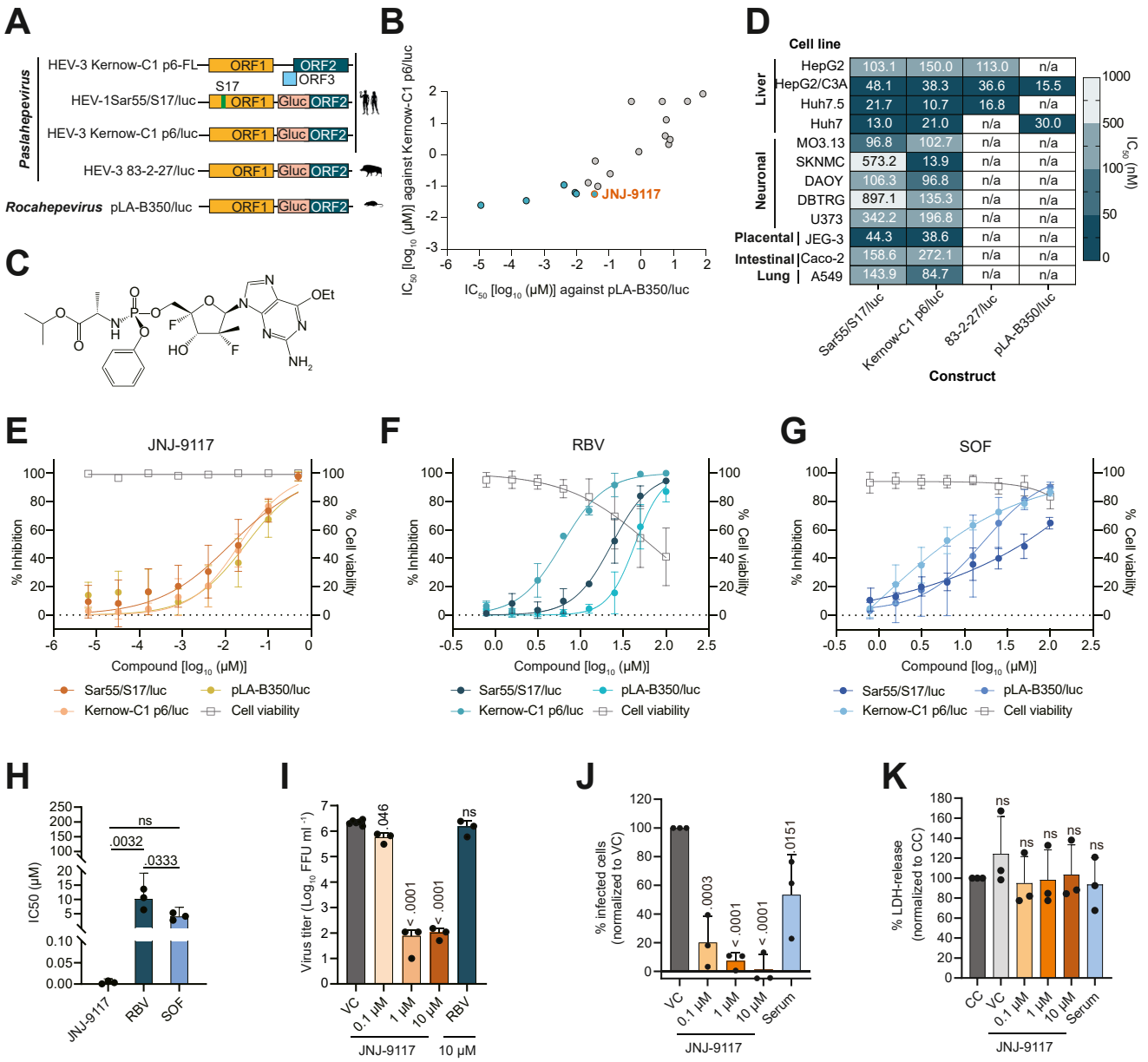

Figure 1. Identification of JNJ-9117 as a potent inhibitor of HEV replication and infection. (*A*) Constructs of different HEV variants used in the in vitro assessments. (*B*) Scatterplot of 50% inhibitory concentration (IC_{50}) values (μmol/L) against the HEV-3 replicon vs those against the rat HEV replicon for tested compounds. (*C*) JNJ-9117 chemical structure. (*D*) Heat map of IC_{50} values (nmol/L) of JNJ-9117 in various cells and against different HEV replicon variants. Mean percentage inhibition of replication for different HEV variants and percentage cytotoxicity of (*E*) JNJ-9117, (*F*) ribavirin (RBV), or (*G*) sofosbuvir (SOF) in Huh7 cells. (*H*) IC_{50} values of JNJ-9117 and ribavirin in HepG2/C3A cells infected with HEV-3 infectious virus. *P* values obtained in ordinary one-way analysis of variance (ANOVA) were corrected with Tukey's multiple comparison. (*I*) Effect of JNJ-9117 and ribavirin on virus titers in HepG2/C3A. (*J*) Antiviral activity of JNJ-9117 against HEV-3 infection in primary human hepatocytes (PHHs); positive control is anti-HEV IgG serum from an HEV-positive patient. (*K*) Cell viability of PHHs during JNJ-9117 treatment, as determined by lactate dehydrogenase (LDH) release into the supernatant in response to cellular damage. Data of *B* and *D*–*G* were analyzed from 3 independent biological replicates. (*I*–*K*) Pooled data of 3 independent experiments were analyzed using ordinary one-way ANOVA with Dunnett's multiple comparison. Data with *error bars* represent mean ± standard deviation or mean + standard deviation. CC, cell control; FFU, focus-forming units; ns, not significant; VC, virus control.

placental JEG-3 (IC_{50}: ~41 nmol/L) cells (Figure 1*D*; dose-response curves shown in Supplementary Figure 1). JNJ-9117 was also active against the HEV-3 83-2-27/luc replicon, a HEV strain from wild boar, which is an important source of zoonotic HEV (Figure 1*D*).

JNJ-9117 also significantly lowered viral RNA levels in the supernatant (Supplementary Figure 2*A*) and the expression of HEV ORF2 (Supplementary Figure 2*C*) in hepatic HepG2/C3A cells transfected with full-length HEV-3 genomic RNA. JNJ-9117 was markedly more effective in

reducing the viral load than ribavirin. JNJ-9117 (100 μmol/L) was nontoxic in transfected cells, whereas a clear toxic effect was noted with ribavirin (50 μmol/L) (Supplementary Figure 2*B*). ORF2 expression was potently reduced by JNJ-9117 (IC_{50}: 3.6 nmol/L) 4 days after HEV-3 infection, which was at concentrations ~2800-fold and ~1100-fold lower than for ribavirin (IC_{50}: 10 μmol/L) and sofosbuvir (IC_{50}: 4.1 μmol/L), respectively (Figure 1*H* and Supplementary Figure 2*D–F*). The potent reduction of ORF2 expression by JNJ-9117 was corroborated by a marked reduction in HEV-3 yield in the presence of JNJ-9117. Viral titers on day 4 postinfection (Figure 1*I*) and viral RNA released into the supernatant on day 10 postinfection (Supplementary Figure 2*H*) were markedly reduced in the presence of 1 or 10 μmol/L JNJ-9117, which were nontoxic (Supplementary Figure 2*G*). Likewise, JNJ-9117 reduced virus yields in rat HEV-infected cell cultures, with the highest concentration (10 μmol/L) suppressing viral RNA replication to almost undetectable levels, even during the 12-day posttreatment period. At 1 μmol/L, JNJ-9117 was able to control rat HEV replication during the treatment period, although rebound occurred when treatment was discontinued (Supplementary Figure 2*I*). In primary human hepatocytes from 3 different donors (Supplementary Table 2) infected with HEV-3, JNJ-9117 inhibited viral replication (80% at 0.1 μmol/L, 93% at 1 μmol/L, and 99% at 10 μmol/L), as measured by ORF2 expression (Figure 1*J* and Supplementary Figure 2*J* and *K*), and none of the concentrations were toxic to the cells (Figure 1*K* and Supplementary Figure 2*L*).

We next compared the effect of JNJ-9117 to that of the replication inhibitor ribavirin and K11777, a cathepsin inhibitor and known entry inhibitor of HEV.[23] While K11777 needed to be present during infection of the cells, addition of JNJ-9117 (and ribavirin) to the infected cells could be delayed for an extended period without losing antiviral activity, which is in line with an inhibitory effect on the intracellular replication process (Figure 2*A* and *B* and Supplementary Figure 2*M*).

JNJ-9117 Acts as a Phosphorylated Guanosine Analogue

JNJ-9117 is a phosphoramidate prodrug of a guanosine analogue that exerts its antiviral effect against HCV through inhibition of the RdRp by its 5′-triphosphate metabolite (JNJ-9117-TP) and this in competition with guanosine-5′-triphosphate (GTP), resulting in chain termination during viral RNA synthesis[22] (Supplementary Figure 3*G*). Although the amino acid sequences of the catalytic site of the HEV1-4, rat HEV, and HCV RdRps are ~25% identical, motifs $DX_{4-5}D$, $GX_{2-3}TX_3N$, and GDD in the catalytic domain of these RdRps (which are imperative for proper catalytic activity[24,25]) are highly conserved (Supplementary Figure 3*A*).

The 3-dimensional structures of the HEV-3 and rat HEV RdRps were predicted using ColabFold[26,27] and subsequently aligned with the crystal structure of the HCV RdRp[28] (Protein Data Bank: 1C2P) (Supplementary Figure 3*B–F*). The HEV-3 RdRp domain superimposes well with that of rat HEV, as indicated by a root mean square deviation of <1 Å for 435 aligned α-carbon atoms. Moreover, the conserved structural motifs in the RdRp catalytic site of HCV and HEV-3 and those in the RdRp catalytic site of HCV and rat HEV also superimpose well with a root mean square deviation of ~1 Å (for 75 and 68 aligned α-carbon atoms, respectively) for both structural alignments, indicating that the HCV and the HEV-3/rat HEV RdRps share a very similar catalytic site architecture (Supplementary Figure 3*F*). The HEV RdRps thus share a common polymerase domain-fold and a well-aligned catalytic active site with that of the HCV RdRp, as indicated by the highly conserved architecture of the marked motifs among these enzymes. It may thus be assumed that JNJ-9117-TP binds most likely to the catalytic site of the RdRp of rat HEV and HEV-3 (and the other HEV genotypes), allowing it to be recognized as a substrate and incorporated into the nascent viral RNA chain by the HEV RdRp, as reported for HCV.[22] Chain termination likely occurs due to steric hindrance caused by the 2′-methyl or 2′,4′-difluoro groups, akin to the mechanism proposed for sofosbuvir.[29,30]

Exogenously added guanosine partially reversed the antiviral activity of JNJ-9117 against HEV-3 replicon replication (Figure 2*C* and *D*), which is expected for a molecule that competes with GTP at the level of the viral polymerase (Supplementary Figure 3*G*). Exogenous guanosine had an even more pronounced effect on the antiviral activity of ribavirin (Figure 2*E*), which corresponds with its mechanism of action against HEV that likely solely relies on the depletion of intracellular GTP pools[31] (Supplementary Figure 3*G*). As anticipated, exogenous guanosine did not affect the antiviral activity of interferon alfa (IFN-α), nor did adenosine reverse the antiviral effect of JNJ-9117 (Supplementary Figure 3*H* and *I*).

To explain the more pronounced antiviral activity in hepatic vs nonhepatic cells, the concentrations of the prodrug (JNJ-9117) and the active metabolite (JNJ-9117-TP) were quantified in Huh7, HepG2/C3A, A549, and Caco-2 cells after 48 or 96 hours of incubation with the prodrug. The active metabolite was most efficiently formed in Huh7 and HepG2/C3A cells, which is consistent with the fact that the anti-HEV activity was also more pronounced in hepatic than in nonhepatic cells (compare Figure 1*D* and Supplementary Figure 4*A* and *B*). The 5′-triphosphate formation was less than proportional with increasing doses, indicating potential saturation of the metabolizing capacity at concentrations of ≥10 μmol/L.[22]

Effectiveness of JNJ-9117 Against Hepatitis E Virus Polymerase Mutants

We next studied whether subgenomic replicons of HEV-3 harboring ribavirin-associated (Y1320H, K1383N, or G1634R[11,32,33]) or sofosbuvir-associated (A1343V[15]) mutations in the RdRp (Supplementary Figure 3*C*) remained sensitive to JNJ-9117. Replicons carrying Y1320H, K1383N, G1634R, K1383N/G1634R, or Y1320H/K1383N/G1634R were equally sensitive to JNJ-9117 as the wild-type HEV-3 replicon (Figure 2*F* and Supplementary Figure 4*C*).

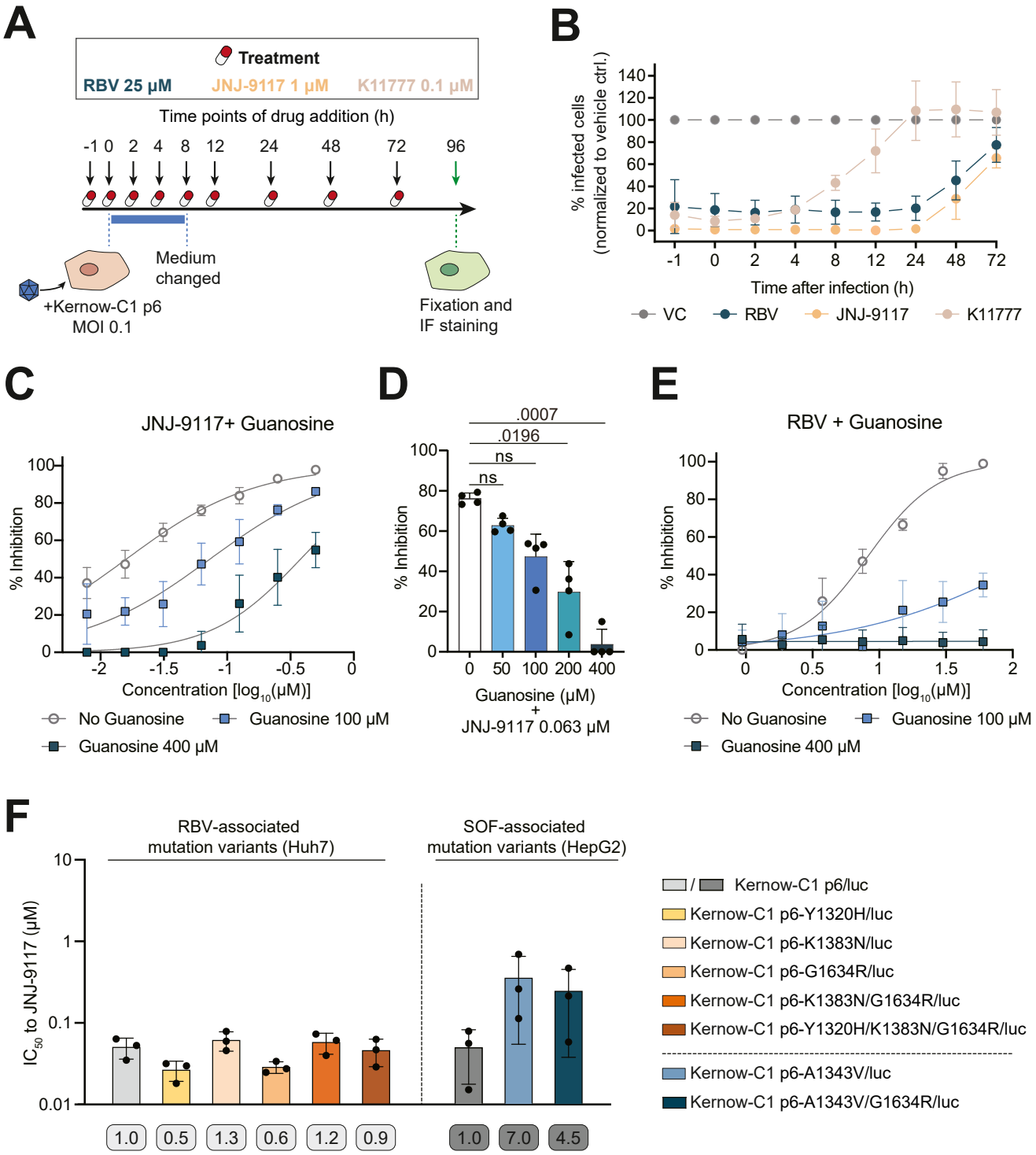

Figure 2. Mode-of-action of JNJ-9117 in vitro. (*A*) Experimental setup of time of drug addition assay. MOI, multiplicity of infection; RBV, ribavirin. (*B*) Inhibitory effect of JNJ-9117 on HEV-3 infection in HepG2/C3A cells when added at the indicated times. At 8 hours postinfection, inoculum was replaced with fresh medium containing drugs. Percentage of infected cells was quantified 96 hours postinfection by immunofluorescence (IF) staining of HEV ORF2. The broad-spectrum viral RNA replication inhibitor ribavirin and the HEV entry inhibitor K11777 served as controls. VC, virus control. (*C*) Dose-response curves of JNJ-9117 (0.5–0.0078 μmol/L) against HEV-3 replicon replication in Huh7 cells under guanosine treatment. (*D*) Percentage inhibition of JNJ-9117 (0.063 μmol/L) under guanosine treatment in Huh7 cells. Statistical analysis was performed using the Kruskal-Wallis test. (*E*) Dose-response curves of ribavirin (60-0.94 μmol/L) against HEV-3 replicon–transfected Huh7 cells under guanosine treatment. Data were obtained from 2 independent experiments. (*F*) Effect of JNJ-9117 on replication of different HEV-3 replicon variants carrying the ribavirin-associated mutations Y1320H, K1383N, G1634R, K1383N/G1634R, Y1320H/K1383N/G1634R or the sofosbuvir (SOF)-associated mutations A1343V and A1343V/G1634R was assessed in Huh7 and HepG2 cells, respectively. IC_{50} fold changes (below the histogram) were determined by comparing the IC_{50} of JNJ-9117 against the different mutant replicon variants to that against the wild-type HEV-3 replicon. Data of *B–D* and *F* were obtained from at least 3 independent experiments. Data with *error bars* represent mean ± standard deviation or mean + standard deviation.

Conversely, a 7.0-fold and 4.5-fold increase in the IC_{50} was observed for the sofosbuvir-associated mutant A1343V and the double A1343V/G1634R mutant compared with the wild-type (Figure 2*F*). The increase in the IC_{50} values was not significantly different among the A1343V and A1343V/G1634R mutants, suggesting that the reduced sensitivity to JNJ-9117 relied on the A1343V mutation (Figure 2*F* and Supplementary Figure 4*D*).

To determine JNJ-9117′s genetic barrier to resistance, rat HEV-infected Huh7 cells were exposed to suboptimal concentrations of JNJ-9117 during 19 consecutive passages (N = 3) (Supplementary Figure 5*A*). Intracellular viral RNA loads determined at the end of each passage were used, when needed, to adjust the concentration in the next passage or to even introduce a treatment pause to avoid virus loss (as happened for sample 3). No noticeable change in the susceptibility to JNJ-9117 was noted, as evidence by the relatively stable intracellular viral RNA load from passage 7 (sample 1) or 9 (sample 2) onward (Supplementary Figure 5*B*).

Sequencing of the RdRp domain in ORF1 of the samples collected at passages 11 and 19 together with the wild-type viral inoculum identified N1525S in the 2 remaining samples at passage 11 (Supplementary Figure 5*C*). However, at passage 19, the mutation had (almost) reverted to the wild-type amino acid. A second change (E1508Q) in the RdRp domain was only found in sample 2 at passage 19 (Supplementary Figure 5*D*). Both changes also emerged in the untreated wild-type sample that was passaged along ("virus control"), thus cannot be considered JNJ-9117–associated (the position of N1525S and E1508Q are marked in red on the predicted rat HEV RdRp structure in Supplementary Figure 5*E*).

To study the potential impact of the identified mutations in the in vitro resistance selection experiment on viral fitness and susceptibility to JNJ-9117, we engineered both the single and double mutants in the background of the wild-type rat HEV subgenomic replicons. None of the mutants resulted in reduced sensitivity to JNJ-9117 (Supplementary Figure 5*G*). Yet, the replication capacity of E1508Q, N1525S, and E1508Q/N1525S increased by a factor 1.9, 2.8, and 4.0, respectively, over that of wild-type (Supplementary Figure 5*F*).

Pharmacokinetics of JNJ-9117 in Rats

The pharmacokinetic profile of JNJ-9117 was evaluated in the liver and plasma of athymic nude rats, which were also used in the rat HEV infection experiments. Rats received a single dose of 200 mg/kg JNJ-9117 (10 mL/kg) by oral gavage and were subsequently humanely killed for collection of plasma and liver samples at 0.25, 0.5, 1, 2, 4, 6, 10, and 24 hours after dosing (n = 3 for each time point). Concentrations of JNJ-9117 (prodrug), its active metabolite 5′-triphosphate (JNJ-9117-TP) and other metabolites, including 5′-monophosphate (JNJ-9117-MP), 5′-diphosphate (JNJ-9117-DP), the parent nucleoside (JNJ-9117-NUC), and the *O*-ethylated parent nucleoside (JNJ-9117-OEt), were determined. High levels of JNJ-9117-TP were achieved in the liver (peak levels at 6 hours postdosing), indicative of good absorption after oral dosing, followed by formation of the active triphosphate in the liver. Triphosphate levels were not measurable in plasma (Table 1 and Supplementary Figure 6*A*).

Prophylactic Antiviral Efficacy of JNJ-9117 in Rats

The effect of JNJ-9117 was subsequently assessed in the HEV infection model in athymic nude rats[20] (Figure 3*A*). Rats were orally treated with JNJ-9117 at 3 different doses (20, 70, or 200 mg/kg/d, twice daily). Control rats were orally treated with vehicle (twice daily; ie, the same dosing frequency as JNJ-9117; negative controls) or ribavirin (at 60 mg/kg, once daily, as previously assessed[21]; positive controls). Based on the pharmacokinetics in rats (this study) and dogs,[22] treatment with JNJ-9117 (and vehicle) was initiated 12 hours before infection. Ribavirin treatment was initiated 2 hours before infection, as described previously.[21] All treatments continued until day 11 postinfection.

Rats were intravenously infected with a diluted liver homogenate stock of rat HEV LA-B350 (containing $\sim 1\times10^6$ viral RNA copies). Viral RNA was quantified in feces (collected every fourth day and at the end point on day 12 postinfection) and organs (liver, intestine, and spleen at end point). No significant weight loss or any other readily observable adverse effects were noted in rats treated with JNJ-9117 or ribavirin (Supplementary Figure 6*B*). Treatment with 70 or 200 mg/kg/d JNJ-9117 resulted in significantly lower viral RNA levels on day 12 postinfection in the feces and liver of HEV-infected rats compared with those in vehicle-treated rats (Figure 3*B*–*D*).

The reduced viral load in the liver of rats treated with 200 mg/kg/d JNJ-9117 was corroborated by a significant decrease in HEV ORF2 expression compared with vehicle-treated rats (Figure 3*E*, *black arrows*). More specifically, all rats in the highest-dosing group had undetectable viral RNA levels in the feces, liver, and spleen (Figure 3*B*–*D* and Supplementary Figure 6*C*). The medium dose of JNJ-9117 significantly reduced viral RNA levels in the liver (by 2.6 $\log_{10}$) and feces (by 1.9 $\log_{10}$), whereas the lowest dose was not efficacious in lowering the viral RNA load in either sample (Figure 3*C* and *D* and Supplementary Figure 6*C*). The antiviral effect of ribavirin was comparable to that of the highest dose of JNJ-9117 in inhibiting viral replication in the studied tissues. For none of the treated groups, a significant drop in the intestinal viral load was noted (Supplementary Figure 6*D*), possibly due to the low viral load in the intestine in the vehicle-treated rats at this stage.

To determine the presence of infectious virus in tissues with viral RNA levels near the lower limit of quantification (LLOQ), virus extracted from a small selection of liver homogenates was used to infect Huh7 cells. The gradually increasing levels of viral RNA released in the medium of inoculated Huh7 cells (Supplementary Figure 6*E*, *left panel*) demonstrate that infectious virus was present in liver

Table 1. Pharmacokinetic Properties of JNJ-9117 and Its Active Metabolites in Plasma and Liver of Athymic Nude Rats

Sample	Cmax (ng/mL)	Tmax (h)	AUC0–24 (ng · h/mL)
Plasma			
Prodrug (JNJ-9117)	2.8	6	16.5
Parent nucleoside (JNJ-9117-NUC)	2200	10	31,000
O-ethylated parent nucleoside (JNJ-9117-OEt)	2010	6	26,500
Liver			
Prodrug (JNJ-9117)	447	0.5	1,580
Monophosphate (JNJ-9117-MP)	27,500	6	329,000
Diphosphate (JNJ-9117-DP)	12,000	6	156,000
Triphosphate (JNJ-9117-TP)	36,900	6	409,000
Parent nucleoside (JNJ-9117-NUC)	28,300	6	430,000
O-ethylated parent nucleoside (JNJ-9117-OEt)	20,500	0.25	57,100

NOTE. JNJ-9117 was orally administered to female athymic nude rats as a solution formulated in polyethylene glycol 400/water (70/30) at 200 mg/kg.
AUC0–24, area under the plasma/liver concentration vs time curve during 24 hours; JNJ-9117-MP, 5'-monophosphate metabolite of JNJ-9117; JNJ-9117-DP, 5'-diphosphate metabolite of JNJ-9117; JNJ-9117-TP, 5'-triphosphate metabolite of JNJ-9117.

samples with HEV RNA levels above the LLOQ but was absent in liver samples with viral RNA levels below the LLOQ (Supplementary Figure 6*E, right panel*). Thus, infectious virus was present in all liver and spleen samples from vehicle-treated rats and in ~50% of the samples from rats treated with 20 mg/kg/d JNJ-9117.

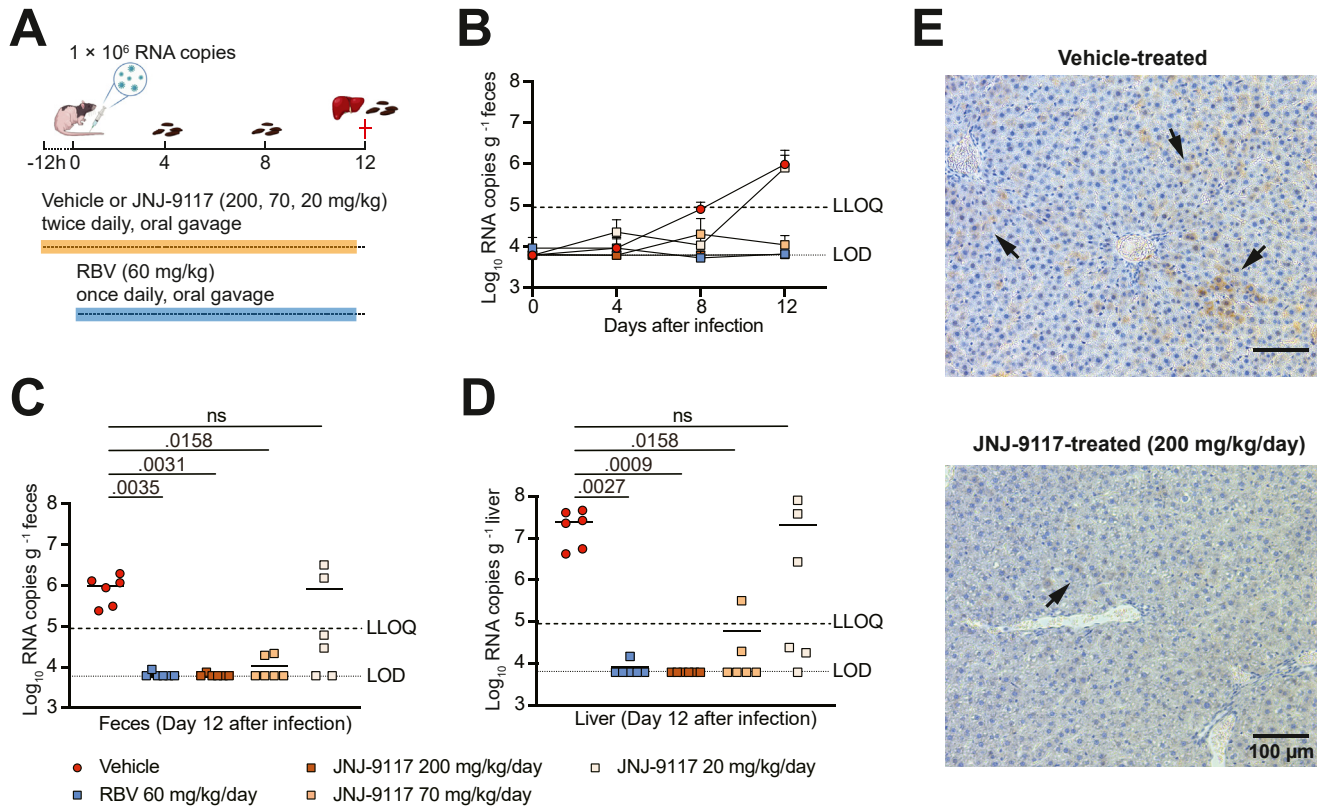

Figure 3. In vivo efficacy of JNJ-9117 on rat HEV replication in a prophylactic setting. (*A*) Schematic of the prophylaxis study. RBV, ribavirin. (*B*) Viral RNA levels in fecal samples collected from rats treated with different compounds (vehicle, ribavirin at 60 mg/kg/d, or JNJ-9117 at 20, 70 or 200 mg/kg/d) at various times postinfection (n = 6 in each group). Data represent mean + standard deviation. ns, not significant. Viral RNA levels in (*C*) feces and (*D*) liver of vehicle- and compound-treated (ie, ribavirin or JNJ-9117) rats on day 12 postinfection. Statistical analysis was performed using the Kruskal-Wallis test. LOD, limit of detection. (*E*) Histologic staining of ORF2 (*black arrows*) in vehicle- and JNJ-9117–treated liver specimen. *Scale bar* = 100 µm.

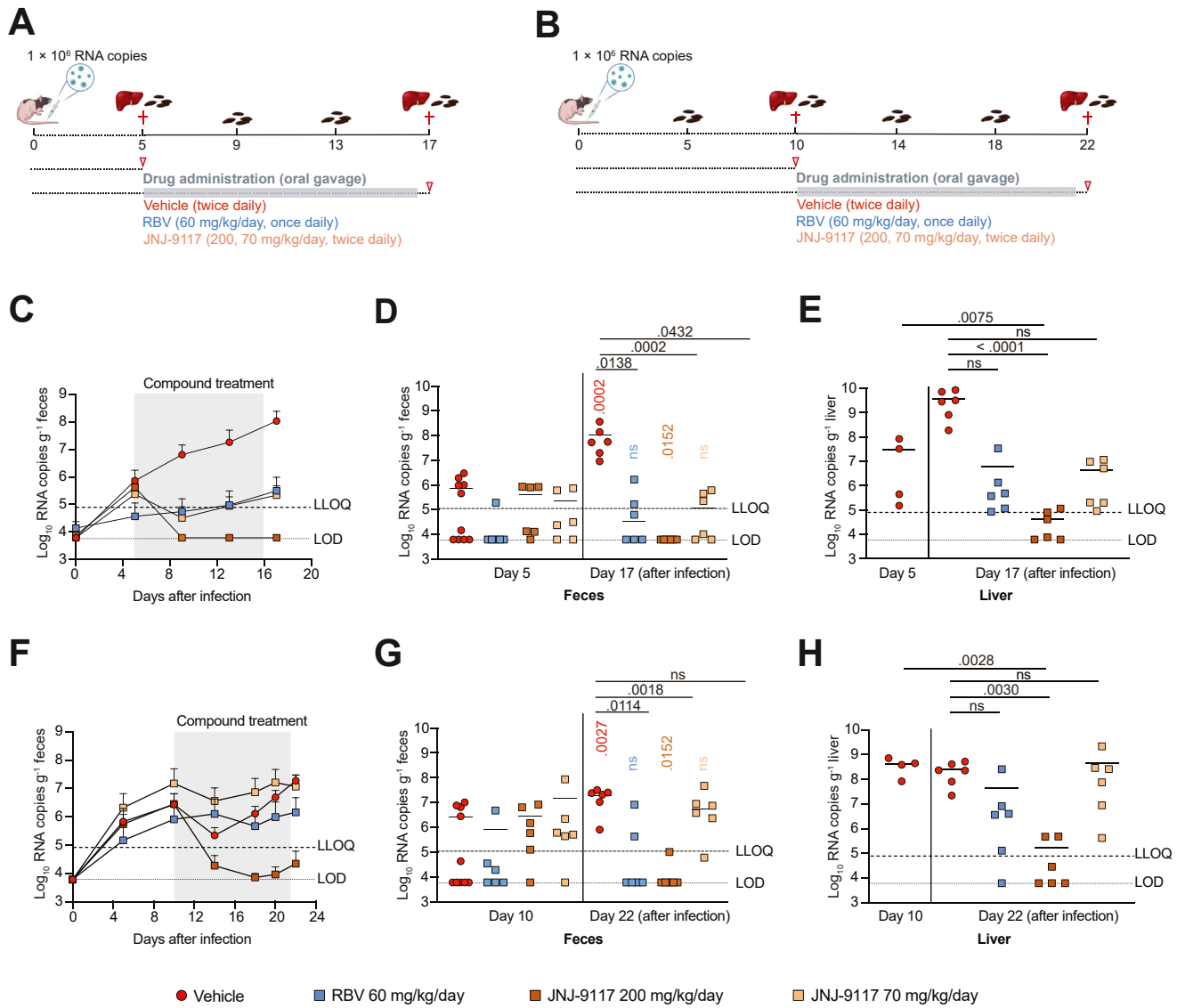

Figure 4. In vivo efficacy of JNJ-9117 on rat HEV replication in a therapeutic setting. (*A* and *B*) Schematic of the therapeutic studies. Vehicle, JNJ-9117 (70 or 200 mg/kg/d, twice daily) and ribavirin (RBV; 60 mg/kg/d, once daily; positive control) treatments started on day 5 or day 10 after rat HEV infection (n = 10 and n = 6 in the vehicle- and compound-treated groups, respectively) and continued for 12 consecutive days. Four rats from the vehicle group were euthanized for viral RNA detection in the liver. The suppressive effect of JNJ-9117 on viral load in the feces with treatment initiation at (*C* and *D*) day 5 or (*F* and *G*) day 10 postinfection. LOD, limit of detection. Viral RNA levels in the liver on (*E*) day 17 or (*H*) day 22 postinfection in the different groups. Statistical analysis was performed using the Kruskal-Wallis test for comparing the treatment groups on (*D* and *E*) day 17 or (*G* and *H*) day 22 postinfection with the respective vehicle group on day 17 and day 22, and for comparing the treatment groups on day 17 and day 22 with the respective vehicle group on (*E*) day 5 and (*H*) day 10. The Mann-Whitney test was used for comparing the day 5 and day 10 results for each group against results for day 17 and day 22, respectively. ns, not significant.

Therapeutic Antiviral Efficacy of JNJ-9117 in Rats

JNJ-9117 efficacy was next assessed on an ongoing HEV infection in athymic nude rats, mimicking a therapeutic setting in humans. The experimental design was essentially the same as in the previous experiment, except that treatment with JNJ-9117 (70 or 200 mg/kg/d, twice daily), ribavirin (60 mg/kg/d, once daily), or vehicle (twice daily) started on day 5 (Figure 4*A*) or day 10 (Figure 4*B*) postinfection. All rats were treated for 12 consecutive days and euthanized on day 17 or day 22 postinfection for treatment start on day 5 or day 10, respectively. A subset of the vehicle rats were euthanized on day 5 or day 10 postinfection for quantification of the viral load at the time treatment was initiated.

On day 5 postinfection, rats had already detectable viral RNA in the feces (half of the rats) and liver (all rats) (Figure 4*C*–*E*), whereas viral RNA levels in the other studied tissues and serum were near or below the LLOQ (Supplementary Figure 7*A*–*C*). On day 17 postinfection, levels in the vehicle-treated rats were (well) above the

LLOQ, with the highest viral load in the liver (9.9 $\log_{10}$ RNA copies/g) and feces (8.6 $\log_{10}$ RNA copies/g). By contrast all rats treated with 200 mg/kg/d JNJ-9117 had undetectable viral RNA levels in their tissues on day 17 postinfection, except the liver (Figure 4*C*–*E* and Supplementary Figure 7*A*–*C*). Levels in the liver were significantly lower (by 4.9 $\log_{10}$) than in vehicle-treated rats on day 17 postinfection, remaining below the LLOQ in most rats. Interestingly, viral RNA levels were even (significantly) lower than those in the tissues on day 5 postinfection.

Virus in liver samples with viral RNA levels above the LLOQ was infectious, as evidenced by the ability to replicate in Huh7 cells (Supplementary Figure 7*D*). The 70 mg/kg/d dose of JNJ-9117 also significantly reduced viral replication in all tissues and serum except the liver (as quantified on day 17 postinfection). On day 10 postinfection, viral RNA levels were well above the LLOQ in all studied tissues of almost all vehicle-treated rats (Figure 4*H* and Supplementary Figure 7*E* and *F*). However, considerable variation was noted in the viral RNA load in feces (and probably also in the other tissues) in the 10 vehicle-treated rats on day 10 postinfection, with 6 rats having viral RNA levels below the LLOQ and 4 rats with average levels of 6.8 $\log_{10}$ RNA copies/g (Figure 4*G*). This variability may be attributable to differences in infection progression, with 4 rats exhibiting robust viral levels by day 10, whereas a delayed onset of infection may have occurred in the other 6 rats, explaining the drop in viral RNA levels in the vehicle group (Figure 4*F*).

Notwithstanding the delayed infection, HEV replicated to peak levels of 7.5 $\log_{10}$ RNA copies/g in the feces and 8.7 $\log_{10}$ RNA copies/g in the liver on day 22 postinfection (Figure 4*G* and *H*). Only the highest dose of JNJ-9117 resulted in significantly lower viral RNA levels in all studied tissues on day 22 postinfection compared with those in the vehicle-treated rats on day 22 postinfection (Figure 4*F*–*H* and Supplementary Figure 7*E*–*G*). Notably, at least 50% of the rats treated with 200 mg/kg/d JNJ-9117 remained negative for viral RNA in the liver until the end of the experiment.

JNJ-9117 is Effective in Chronically Infected Rats

To study whether JNJ-9117 is also effective in chronically infected animals, rats were fecal-orally infected 60 days before start of treatment. Viral RNA copies in the feces increased steadily from day 15 onward to reach levels of ~9 $\log_{10}$ RNA copies/g by day 40, after which a plateau phase was reached (Figure 5). Approximately 20 days after reaching this plateau, treatment was initiated at 200 mg/kg/d twice daily for 10 consecutive days, except for rat 2, for which the dose was lowered to 150 mg/kg/d twice daily on days 9 and 10 posttreatment. On day 10 posttreatment (ie, day 70 postinfection), viral RNA levels in the feces of the 3 rats had decreased by ~4 $\log_{10}$ RNA copies/g. Thus, JNJ-9117 is highly effective in curbing a chronic HEV infection.

Prolonged Suboptimal Dosing in Chronically Infected Rats Does Not Result in Drug Resistance

We next explored whether JNJ-9117, once it achieved a drop in fecal viral loads to (or below) the LLOQ, would result in the selection of drug-resistant variants when treatment was continued with suboptimal dosing in the subsequent weeks. To that end, twice-daily dosing was reduced, and viral RNA levels in the feces of each individual rat were quantified every 2 to 3 days. Where needed (depending on the trend in the viral RNA levels), the dose was slightly increased or decreased (Figure 5). This allowed for control of the infection (with viral RNA levels being 3–4 $\log_{10}$ below those at the start of treatment) until days 125 and 130 postinfection. At end point, N1525S, which is not linked to resistance as demonstrated in the in vitro resistance selection, was identified in the feces of all 3 rats (and on day 109 postinfection in rat 2). N1525S was not detected in fecal samples before start of treatment (Supplementary Figure 8). Amino acid changes E305G and P605L were identified at end point in the feces of rats 1 and 2 but were also already detected (albeit not dominant) at the start of treatment (day 60 postinfection) and are most likely thus not drug induced. Furthermore, P134A, F555S, and V558A were only detected in the feces of 1 rat, all of which were also present in fecal samples collected at the start of treatment, making them unlikely to be related to drug susceptibility.

The Antiviral Effect of JNJ-9117 Is Additive When Combined With Ribavirin

Lastly, we studied the antiviral effect of JNJ-9117 on HEV-1, HEV-3, and rat HEV replicon replication when combined with ribavirin or sofosbuvir (Supplementary Figure 9). ZIP synergy scores were well above 5 for the combination JNJ-9117/ribavirin across all 3 replicon models (Supplementary Figure 9*A*–*C*), indicative of an additive effect, as also illustrated by the dose-response interaction matrices (Supplementary Figure 9*D*–*F*). Within certain concentration ranges, a synergistic effect of the combination JNJ-9117/ribavirin was noted, as shown by the dark orange-colored areas in Supplementary Figure 9*A*–*C*. The combination JNJ-9117/sofosbuvir was mostly slightly antagonistic (Supplementary Figure 9*G*–*L*).

We then assessed the combined effect of JNJ-9117 and ribavirin in infected rats. Animals were treated with combinations of suboptimal doses of JNJ-9117 (30 or 40 mg/kg/d, twice daily) and ribavirin (20 or 30 mg/kg/d, once daily). Treatment started 2 hours before infection and continued for 12 consecutive days (Figure 6*A*). No adverse effects or body weight loss were observed in any of the groups (Figure 6*B*). Ribavirin and JNJ-9117, when given as monotherapy, resulted in incomplete reduction of viral RNA loads in the feces and liver, as expected. All JNJ-9117/ribavirin combinations, except the 30 mg/kg/d JNJ-9117 plus 20 mg/kg/d ribavirin combination, efficiently reduced viral RNA levels in the feces and liver and this to nearly undetectable levels (Figure 6*C*–*J*).

Discussion

Globally, HEV is the leading etiologic agent of acute viral hepatitis, accounting annually for up to 44,000 deaths,[1,34]

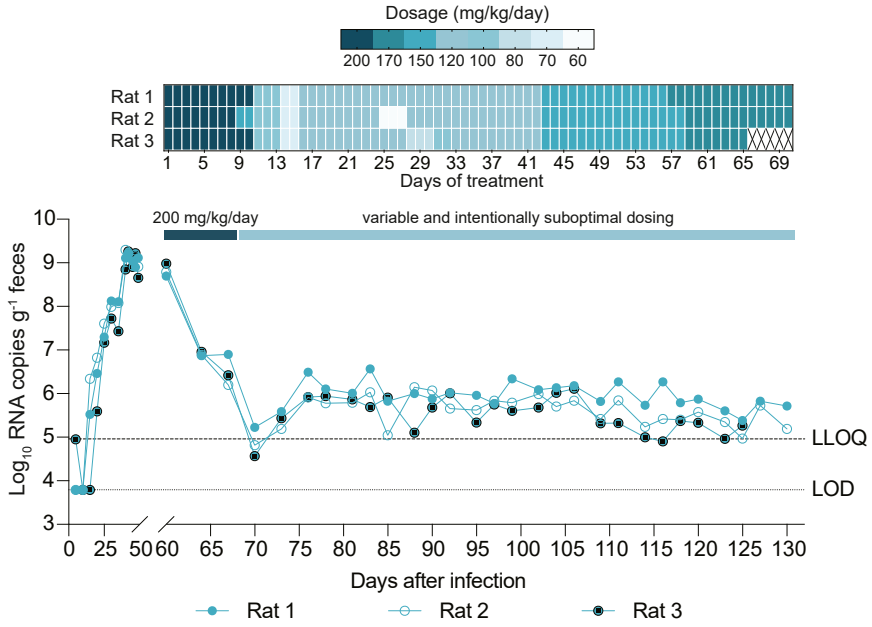

Figure 5. High efficacy and barrier to resistance of JNJ-9117 in a chronic HEV infection model. After rat HEV infection, viral RNA copies in feces of rats (N = 3) increased to a plateau phase by day 40 postinfection, which was ~20 days before JNJ-9117 treatment (ie, on day 60 postinfection) of the chronically infected rats was started. Once viral levels had declined to (nearly) undetectable, the dose was reduced to allow virus rebound. Viral RNA levels in feces of individual rats were quantified every 2 to 3 days, and when required, the dose was slightly increased or decreased to maintain a low level of viral RNA in the feces; a condition that may favor the selection of drug-resistant variants. Rat 3 was humanely killed on day 125 postinfection due to low viral load detected in feces on day 123 postinfection. LOD, limit of detection.

The current off-label monotherapy treatment with ribavirin in patients with chronic hepatitis E can be associated with severe adverse effects and a frequently inadequate sustained virologic response.[11,32,35] Pegylated–IFN-α is also considered in liver transplant patients who are refractory to ribavirin; yet, this treatment is also associated with important adverse effects.[36] Ribavirin and pegylated–IFN-α are both contraindicated during pregnancy, thus leaving no therapeutic options in case of life-threatening HEV infections in pregnant women. There is hence a pressing need for (a) safe and efficacious antiviral drug(s) for the treatment of severe HEV infections.[4]

We and others demonstrated that the HCV polymerase inhibitor sofosbuvir inhibits HEV replication in cell culture; yet, the antiviral potency is insufficient to result in a pronounced clinical benefit.[13,14] We therefore explored whether a series of sugar-modified guanosine analogues, developed in the context of an earlier HCV program, can inhibit HEV replication. From this series, JNJ-9117 exhibited robust in vitro pangenotype antiviral activity against HEV and this in various human hepatic cells, including primary human hepatocytes. Although JNJ-9117 is not the most potent in this series, it exhibits a more favorable profile (ie, robust triphosphate formation in human hepatocytes and good stability properties) than the more potent compounds. The nucleoside was also active against HEV in various extrahepatic cells, including neuronal, intestinal, lung, and placental cells, which is particularly of interest given the association of HEV with extrahepatic clinical manifestations and the ability of the virus to cross the placental barrier.[37,38]

There is a high level of conservation between 3 crucial motifs in the catalytic site of the HCV and HEV polymerases. It is therefore reasonable to assume that JNJ-9117 inhibits HEV replication by the same mode of action by which it inhibits HCV replication,[22] which is through the incorporation of its 5′-triphosphate metabolite (JNJ-9117-TP) instead of GTP during viral RNA synthesis, resulting in chain termination. Because a HEV polymerase assay is not available, we are unable to directly study an inhibitory effect of JNJ-9117-TP on this enzyme. Our observation that exogenously added guanosine reverted the anti-HEV activity of JNJ-9117 provides further evidence that the HEV polymerase is the likely molecular target of JNJ-9117. The finding that guanosine was more efficient in reversing the anti-HEV activity of ribavirin than that of JNJ-9117 corroborates the fact that ribavirin predominantly inhibits HEV replication via depletion of intracellular GTP pools.[31]

JNJ-9117 has a favorable pharmacokinetic and safety profile, both in rats (this study) and dogs,[22] and we therefore explored its potential for the treatment of HEV infections in a rat HEV infection model. In this model, JNJ-9117 reduced viral loads in the liver and other tissues to almost undetectable if treatment was initiated before the infection. Even in a therapeutic setting in which treatment was initiated as late as 10 days postinfection, a rapid and significant reduction in viral RNA levels in the feces was observed within 4 days of treatment. Furthermore, the molecule was able to reduce viral loads in the liver (12 days later at end point) to low and even undetectable levels.

We next wanted to explore whether JNJ-9117 is also effective against an established or chronic infection. When treatment was initiated at day 60 postinfection, which is ~20 days after viral RNA levels in the feces reached a high plateau, the molecule yielded a remarkable drop in viral replication (ie, ~4 $\log_{10}$ within 10 days). Complete viral RNA elimination in the feces, and possibly in the liver, may likely be expected with continued treatment at the same dosage.

When we explored the combined antiviral effect of intentionally selected suboptimal doses of both JNJ-9117 and ribavirin in the rat model, a pronounced antiviral effect was observed. This may suggest that in case such a

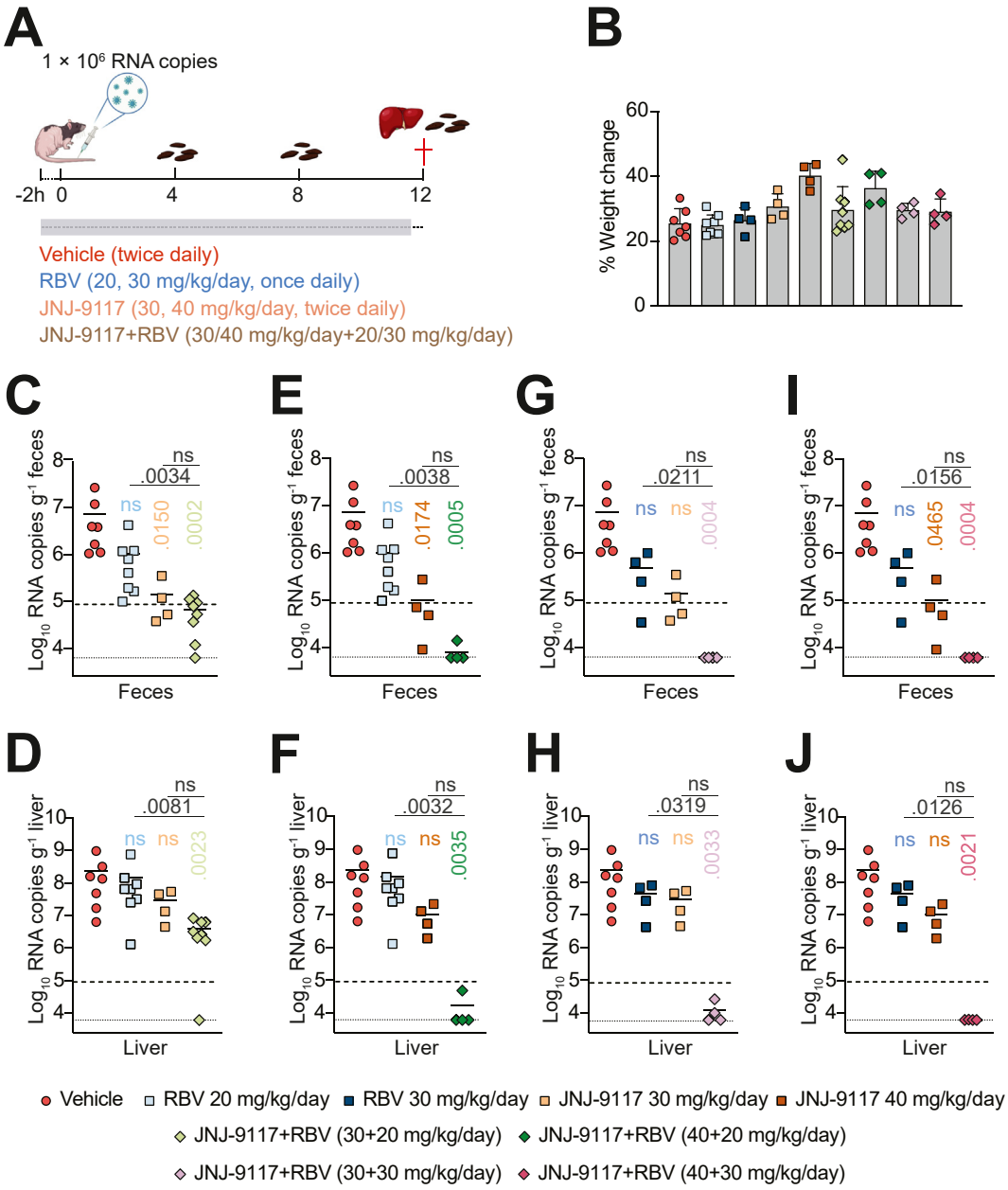

Figure 6. Efficacy of the combination of JNJ-9117 and ribavirin (RBV) in rat HEV-infected rats. (*A*) Schematic of the antiviral combination studies. Rats received vehicle (n = 7 in 2 independent experiments), single-treatment of ribavirin 20 mg/kg/d, once daily (n = 8 in 2 independent experiments), ribavirin at 30 mg/kg/d, once daily, or JNJ-9117 at 30 or 40 mg/kg/d, twice daily (n = 4 each), or dual-treatment using 4 different combinations of the monotreatment doses of ribavirin and JNJ-9117 described above (n = 8 for the combination JNJ-9117–30 mg/kg with ribavirin–20 mg/kg, 2 independent experiments; n = 4 each for all the other combination groups). Treatment continued for 12 consecutive days. Rats were infected with rat HEV liver homogenate 2 hours after treatment start. (*B*) Percentage weight change on day 12 postinfection relative to the initial weight on day 0 post-infection. Viral RNA levels in (*C*, *E*, *G*, and *I*) feces and (*D*, *F*, *H*, and *J*) liver in vehicle- and compound-treated rats on day 12 postinfection. Statistical analysis was performed using the Kruskal-Wallis test, followed by the Dunn's post hoc test. The *bottom dashed line* in the graphs represents the limit of detection (LOD); the *top dashed line* represents the lower limit of quantification (LLOQ). ns, not significant.

combination would be used in patients with chronic HEV infections, it may result in a pronounced antiviral effect while permitting dose reductions. This may allow the adverse effects of ribavirin to be minimized. Such a combination will likely also avoid the emergence of ribavirin escape variants.

We were unable to select for JNJ-9117–resistant variants after long-term in vitro passaging of HEV in the presence of JNJ-9117 (19 passages; ~80 days). We then explored whether long-term treatment with intentionally selected suboptimal doses resulted in the emergence of drug-resistance variants in the chronic rat HEV infection model.

The molecule effectively controlled viral replication throughout the entire treatment period under this condition, and no escape mutations were detected. Thus, JNJ-9117 has a high genetic barrier to drug resistance, a characteristic that is of importance in the treatment of chronic viral infections. Interestingly HEV-3 replicons carrying substitutions Y1320H, K1383N, or G1634R that are associated with loss of ribavirin efficacy in patients[11,12,39] remained sensitive to JNJ-9117. Conversely, viruses carrying the sofosbuvir-associated substitution A1343V (either or not in combination with G1634R) had a reduced sensitivity to JNJ-9117. These results indicate that patients with chronic hepatitis E that are refractory to treatment with ribavirin may be expected to be fully susceptible to JNJ-9117. Contrarily, JNJ-9117 may possibly be less efficacious in patients that carry sofosbuvir-resistant HEV.

Taken together, we identified JNJ-9117 as a highly potent pangenotype inhibitor of HEV. The observed pangenotype activity indicates that antiviral activity may also be expected against other HEVs within the *Orthohepevirinae* subfamily, including those circulating in swine, camels, rabbits, and wild boar, all of which serve as potential zoonotic reservoirs for HEV.[40,41]

JNJ-9117 underwent a randomized, double-blind, placebo-controlled phase I clinical study (ClinicalTrials.gov, NCT03253471), in which single ascending dose data were generated using daily doses of up to 200 mg to assess the safety, tolerability, and pharmacokinetics of the orally administered drug. JNJ-9117 shows an acceptable safety and pharmacokinetic profile at the highest dose tested, with no relevant clinical safety signs in this single ascending dose study.[16] Thus, JNJ-9117 is an excellent candidate for further clinical development, such as assessment in a multiple ascending dose phase I study, evaluation in preclinical models for pregnant women, for the treatment of life-threatening HEV infections.

Supplementary Material

Note: To access the supplementary material accompanying this article, visit the online version of *Gastroenterology* at www.gastrojournal.org, and at https://dx.doi.org/10.1053/j.gastro.2024.10.043.

References

1. World Health Organization. Fact sheets. Hepatitis E. 20 July 2023. Available at: https://www.who.int/news-room/fact-sheets/detail/hepatitis-e. Accessed March 11, 2024.
2. World Health Organization. Disease Outbreak News. Acute hepatitis E—South Sudan. 5 May 2023. Available at: https://www.who.int/emergencies/disease-outbreak-news/item/2023-DON466. Accessed March 11, 2024.
3. Desai AN, Mohareb AM, Elkarsany MM, et al. Viral hepatitis E outbreaks in refugees and internally displaced populations, sub-Saharan Africa, 2010-2020. Emerg Infect Dis 2022;28:1074–1076.
4. Kirkwood CD, Dobscha KR, Steele AD. Hepatitis E should be a global public health priority: recommendations for improving surveillance and prevention. Expert Rev Vaccines 2020;19:1129–1140.
5. Damiris K, Meybodi MA, Niazi M, et al. Hepatitis E in immunocompromised individuals. World J Hepatol 2022;14:482–494.
6. Navaneethan U, Al Mohajer M, Shata MT. Hepatitis E and pregnancy: understanding the pathogenesis. Liver Int 2008;28:1190–1199.
7. Nelson KE, Labrique AB, Kmush BL. Epidemiology of genotype 1 and 2 hepatitis E virus infections. Cold Spring Harb Perspect Med 2019;9:a031732.
8. Smith DB, Izopet J, Nicot F, et al. Update: proposed reference sequences for subtypes of hepatitis E virus (species *Orthohepevirus A*). J Gen Virol 2020;101:692–698.
9. Reuter G, Boros Á, Pankovics P. Review of Hepatitis e virus in rats: evident risk of species *Orthohepevirus C* to human zoonotic infection and disease. Viruses 2020;12:1148.
10. **Øverbø J, Aziz A**, Zaman K, et al. Immunogenicity and safety of a two-dose regimen with hepatitis E virus vaccine in healthy adults in rural Bangladesh: a randomized, double-blind, controlled, phase 2/pilot trial. Vaccine 2023;41:1059–1066.
11. **Debing Y, Ramière C**, Dallmeier K, et al. Hepatitis E virus mutations associated with ribavirin treatment failure result in altered viral fitness and ribavirin sensitivity. J Hepatol 2016;65:499–508.
12. Debing Y, Gisa A, Dallmeier K, et al. A mutation in the hepatitis E virus RNA polymerase promotes its replication and associates with ribavirin treatment failure in organ transplant recipients. Gastroenterology 2014;147:1008–1011.e7.
13. Dao Thi VL, Debing Y, Wu X, et al. Sofosbuvir inhibits hepatitis E virus replication in vitro and results in an additive effect when combined with ribavirin. Gastroenterology 2016;150:82–85.e4.
14. Cornberg M, Pischke S, Müller T, et al. Sofosbuvir monotherapy fails to achieve HEV RNA elimination in patients with chronic hepatitis E—The HepNet SofE pilot study. J Hepatol 2020;73:696–699.
15. **Gömer A, Klöhn M, Jagst M**, et al. Emergence of resistance-associated variants during sofosbuvir treatment in chronically infected hepatitis E patients. Hepatology 2023;78:1882–1895.
16. National Library of Medicine. ClinicalTrials.gov ID NCT03253471. A First in Human Study of AL-611 in Healthy Volunteers and Patients With Hepatitis C Virus Infection. Available at: https://clinicaltrials.gov/study/NCT03253471. Accessed March 11, 2024.
17. Shukla P, Nguyen HT, Faulk K, et al. Adaptation of a genotype 3 hepatitis E virus to efficient growth in cell culture depends on an inserted human gene segment acquired by recombination. J Virol 2012;86:5697–5707.
18. Emerson SU, Zhang M, Meng XJ, et al. Recombinant hepatitis E virus genomes infectious for primates: importance of capping and discovery of a cis-reactive element. Proc Natl Acad Sci U S A 2001;98:15270–15275.
19. Shiota T, Li T-C, Yoshizaki S, et al. The hepatitis E virus capsid C-terminal region is essential for the viral life cycle: implication for viral genome encapsidation and particle stabilization. J Virol 2013;87:6031–6036.

20. Debing Y, Mishra N, Verbeken E, et al. A rat model for hepatitis E virus. Dis Model Mech 2016;9:1203–1210.
21. Zhang X, Cremers N, Hendrickx S, et al. Establishment of a robust rat hepatitis E virus fecal-oral infection model and validation for antiviral studies. Antiviral Res 2023; 216:105670.
22. Wang G, Dyatkina N, Prhavc M, et al. Synthesis and anti-HCV activity of sugar-modified guanosine analogues: discovery of AL-611 as an HCV NS5B polymerase inhibitor for the treatment of chronic hepatitis C. J Med Chem 2020;63:10380–10395.
23. **Klöhn M, Burkard T**, Janzen J, et al. Targeting cellular cathepsins inhibits hepatitis E virus entry. Hepatology 2024;80:1239–1251.
24. Gorbalenya AE, Pringle FM, Zeddam JL, et al. The palm subdomain-based active site is internally permuted in viral RNA-dependent RNA polymerases of an ancient lineage. J Mol Biol 2002;324:47–62.
25. Venkataraman S, Prasad BVLS, Selvarajan R. RNA dependent RNA polymerases: insights from structure, function and evolution. Viruses 2018;10:76.
26. **Jumper J, Evans R, Pritzel A**, et al. Highly accurate protein structure prediction with AlphaFold. Nature 2021; 596:583–589.
27. Mirdita M, Schütze K, Moriwaki Y, et al. ColabFold: making protein folding accessible to all. Nat Methods 2022;19:679–682.
28. Lesburg CA, Cable MB, Ferrari E, et al. Crystal structure of the RNA-dependent RNA polymerase from hepatitis C virus reveals a fully encircled active site. Nat Struct Biol 1999;6:937–943.
29. **De Clercq E, Li G**. Approved antiviral drugs over the past 50 years. Clin Microbiol Rev 2016;29:695–747.
30. Maheden K, Todd B, Gordon CJ, et al. Inhibition of viral RNA-dependent RNA polymerases with clinically relevant nucleotide analogs. Enzymes (Essen) 2021;49:315–354.
31. Debing Y, Emerson SU, Wang Y, et al. Ribavirin inhibits in vitro hepatitis E virus replication through depletion of cellular GTP pools and is moderately synergistic with alpha interferon. Antimicrob Agents Chemother 2014;58:267–273.
32. Todt D, Gisa A, Radonic A, et al. In vivo evidence for ribavirin-induced mutagenesis of the hepatitis E virus genome. Gut 2016;65:1733–1743.
33. Wang B, Mahsoub HM, Li W, et al. Ribavirin treatment failure-associated mutation, Y1320H, in the RNA-dependent RNA polymerase of genotype 3 hepatitis E virus (HEV) enhances virus replication in a rabbit HEV infection model. mBio 2023;14:e0337222.
34. Kamar N, Izopet J, Pavio N, et al. Hepatitis E virus infection. Nat Rev Dis Primers 2017;3:17086.
35. Lhomme S, Kamar N, Nicot F, et al. Mutation in the hepatitis E virus polymerase and outcome of ribavirin therapy. Antimicrob Agents Chemother 2015;60:1608–1614.
36. Kamar N, Rostaing L, Abravanel F, et al. Pegylated interferon-alpha for treating chronic hepatitis E virus infection after liver transplantation. Clin Infect Dis 2010; 50:e30–e33.
37. Rawla P, Raj JP, Kannemkuzhiyil AJ, et al. A systematic review of the extra-hepatic manifestations of hepatitis E virus infection. Med Sci (Basel) 2020;8:9.
38. Gouilly J, Chen Q, Siewiera J, et al. Genotype specific pathogenicity of hepatitis E virus at the human maternal-fetal interface. Nat Commun 2018;9:4748.
39. Todt D, Walter S, Brown RJP, et al. Mutagenic effects of ribavirin on hepatitis E virus-viral extinction versus selection of fitness-enhancing mutations. Viruses 2016;8:283.
40. Aslan AT, Balaban HY. Hepatitis E virus: epidemiology, diagnosis, clinical manifestations, and treatment. World J Gastroenterol 2020;26:5543–5560.
41. Grange ZL, Goldstein T, Johnson CK, et al. Ranking the risk of animal-to-human spillover for newly discovered viruses. Proc Natl Acad Sci U S A 2021;118: e2115409118.

Author names in bold designate shared co-first authorship.

Received June 14, 2024. Accepted October 21, 2024.

Correspondence
Address correspondence to: Johan Neyts, PhD, KU Leuven Department of Microbiology, Immunology and Transplantation, Rega Institute for Medical Research, Virology, Antiviral Drug & Vaccine Research Group, Herestraat 49, 3000 Leuven, Belgium. e-mail: johan.neyts@kuleuven.be; or Eike Steinmann, PhD, Department of Molecular and Medical Virology, Ruhr University Bochum, Gebäude MA 6. Etage, Universitätsstrasse 150, 44780 Bochum, Germany. e-mail: eike.steinmann@ruhr-uni-bochum.de; or Anil Koul, PhD, Johnson and Johnson Innovative Medicine, Turnhoutseweg 30, 2340 Beerse, Belgium. e-mail: akoul@its.jnj.com; or Suzanne J.F. Kaptein, PhD, KU Leuven Department of Microbiology, Immunology and Transplantation, Rega Institute for Medical Research, Virology, Antiviral Drug & Vaccine Research Group, Herestraat 49, 3000 Leuven, Belgium. e-mail: suzanne.kaptein@kuleuven.be.

Acknowledgments
The authors thank Ralf Bartenschlager (Heidelberg University, Heidelberg, Germany), Lieve Naesens (KU Leuven Rega Institute, Leuven, Belgium), and Luc Verschaeve (formerly at the Scientific Institute of Public Health, Brussels, Belgium) for kindly providing the Huh7, Caco-2, and HepG2/C3A cells, respectively. The authors thank Suzanne Emerson (formerly at National Institute of Allergy and Infectious Diseases at the National institutes of Health, Bethesda, MD) for generously providing the Sar55/S17/luc, Kernow-C1 p6, Kernow-C1 p6/luc, and rat HEV LA-B350 strain and Takaji Wakita (National Institute of Infectious Diseases, Tokyo, Japan) for kindly providing the 83-2-27 strain. The authors also thank Rainer G. Ulrich for kindly providing the anti–HEV-ORF2 protein antibody, Niels Cremers, Katrien Geerts, Stijn Hendrickx, and the staff at the Rega animal facility at KU Leuven for technical assistance, and Michael Engelmann for technical assistance. Figures were generated using BioRender.com, mindthegraph.com, and Adobe Illustrator.

Johan Neyts, Eike Steinmann, and Anil Koul contributed equally to this work.

CRediT Authorship Contributions
Xin Zhang, PhD (Conceptualization: Equal; Data curation: Equal; Formal analysis: Lead; Investigation: Lead; Methodology: Lead; Validation: Lead; Visualization: Lead; Writing – original draft: Equal)

Mara Klöhn, PhD (Conceptualization: Equal; Data curation: Equal; Formal analysis: Equal; Investigation: Equal; Methodology: Equal; Software: Equal; Validation: Equal; Writing – original draft: Equal; Writing – review & editing: Equal)

Sivi Ouwerkerk-Mahadevan, PhD (Conceptualization: Supporting; Data curation: Supporting; Formal analysis: Supporting; Methodology: Supporting; Validation: Supporting; Writing – original draft: Supporting; Writing – review & editing: Supporting)

Michelle Jagst, MSc (Data curation: Supporting; Formal analysis: Supporting; Investigation: Supporting; Methodology: Supporting; Validation: Supporting; Writing – original draft: Supporting)

Liesbeth Vereyken, BSc (Conceptualization: Supporting; Data curation: Supporting; Formal analysis: Supporting; Methodology: Supporting; Writing – review & editing: Supporting)

Peter Verboven, BSc (Conceptualization: Supporting; Data curation: Supporting; Formal analysis: Supporting; Methodology: Supporting; Writing – review & editing: Supporting)

Quinten Goovaerts, MSc (Conceptualization: Supporting; Data curation: Supporting; Formal analysis: Supporting; Software: Equal; Writing – review & editing: Supporting)

Daniel Todt, PhD (Conceptualization: Supporting; Methodology: Supporting; Software: Supporting; Writing – review & editing: Supporting)

Tim H. M. Jonckers, PhD (Conceptualization: Supporting; Funding acquisition: Supporting; Investigation: Supporting; Project administration: Equal; Writing – review & editing: Supporting)

Lotte Coelmont, PhD (Funding acquisition: Equal; Project administration: Equal; Writing – review & editing: Supporting)

Helen Fletcher, PhD (Resources: Equal; Supervision: Supporting; Writing – review & editing: Supporting)

Kalyan Das, PhD (Supervision: Supporting; Writing – review & editing: Supporting)

Kirandeep Samby, PhD (Conceptualization: Supporting; Project administration: Supporting; Resources: Supporting; Supervision: Supporting; Writing – review & editing: Supporting)

Johan Neyts, PhD (Conceptualization: Equal; Funding acquisition: Lead; Project administration: Equal; Resources: Lead; Supervision: Equal; Writing – review & editing: Equal)

Eike Steinmann, PhD (Funding acquisition: Equal; Project administration: Equal; Supervision: Equal; Writing – review & editing: Equal)

Anil Koul, PhD (Conceptualization: Equal; Investigation: Equal; Resources: Lead; Supervision: Equal; Writing – review & editing: Supporting)

Suzanne J. F. Kaptein, PhD (Investigation: Lead; Methodology: Lead; Resources: Lead; Supervision: Lead; Writing – original draft: Equal; Writing – review & editing: Lead)

Conflicts of interest

These authors disclose the following: Sivi Ouwerkerk-Mahadevan, Liesbeth Vereyken, Peter Verboven, Tim H. M. Jonckers, Helen Fletcher, Kirandeep Samby, and Anil Koul are full-time employees of Janssen and potential stockholders of Johnson and Johnson. Tim H.M. Jonckers is one of the co-inventors on patent application W02021/209419 A, reporting on the discovery of a series of antiviral molecules for the treatment of hepatitis E. The remaining authors disclose no conflicts.

Funding

Xin Zhang was supported by the China Scholarship Council (grant no. 201906170033). Quinten Goovaerts acknowledges financial support from the Research Foundation—Flanders (FWO-Vlaanderen; doctoral fellowship grant number 1162823N).

Data Availability

Supplementary Materials are provided with this article. Data, analytic methods, and study materials in this study are available from the corresponding author upon reasonable request. GenBank accession number: JQ679013, AF444002, AB740232, KM516906.

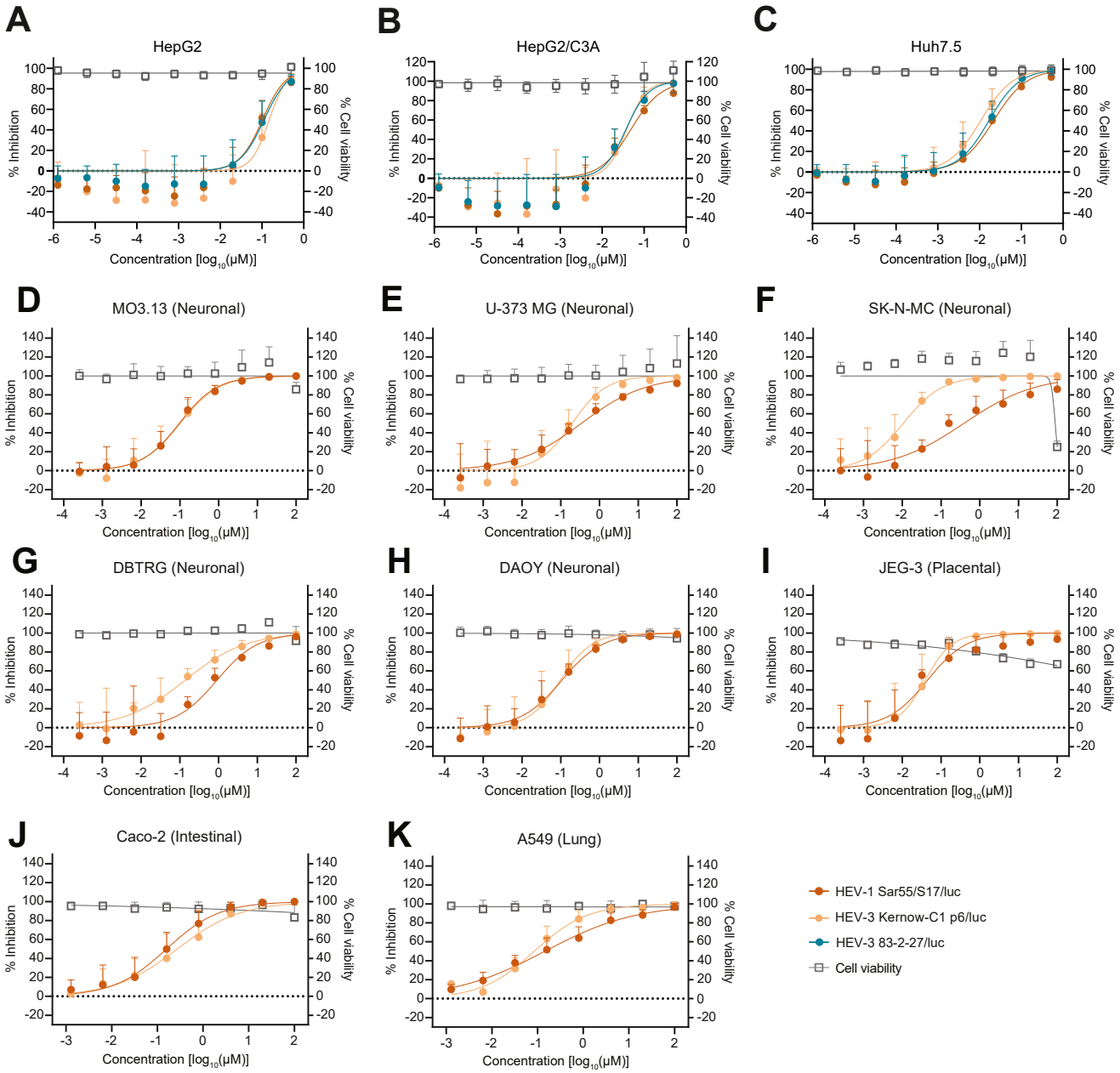

Supplementary Figure 1. Pangenotype inhibition of HEV replication by JNJ-9117 in different cell lines. Dose-dependent inhibition effect of JNJ-9117 on HEV replication against HEV-1 Sar55/S17/luc, HEV-3 Kernow-C1 p6/luc, or HEV-3 83-2-27/luc in the hepatoma cells (*A*) HepG2, (*B*) HepG2/C3A, and (*C*) Huh7.5; the neuronal cells (*D*) MO3.13, (*E*) U-373 MG, (*F*) SK-N-MC, (*G*) DBTRG, and (*H*) DAOY; the (*I*) placenta cells JEG-3, (*J*) the intestinal Caco-2 cells, and (*K*) the lung A549 cells. Data represent mean + standard deviation from 3 independent biological replicates.

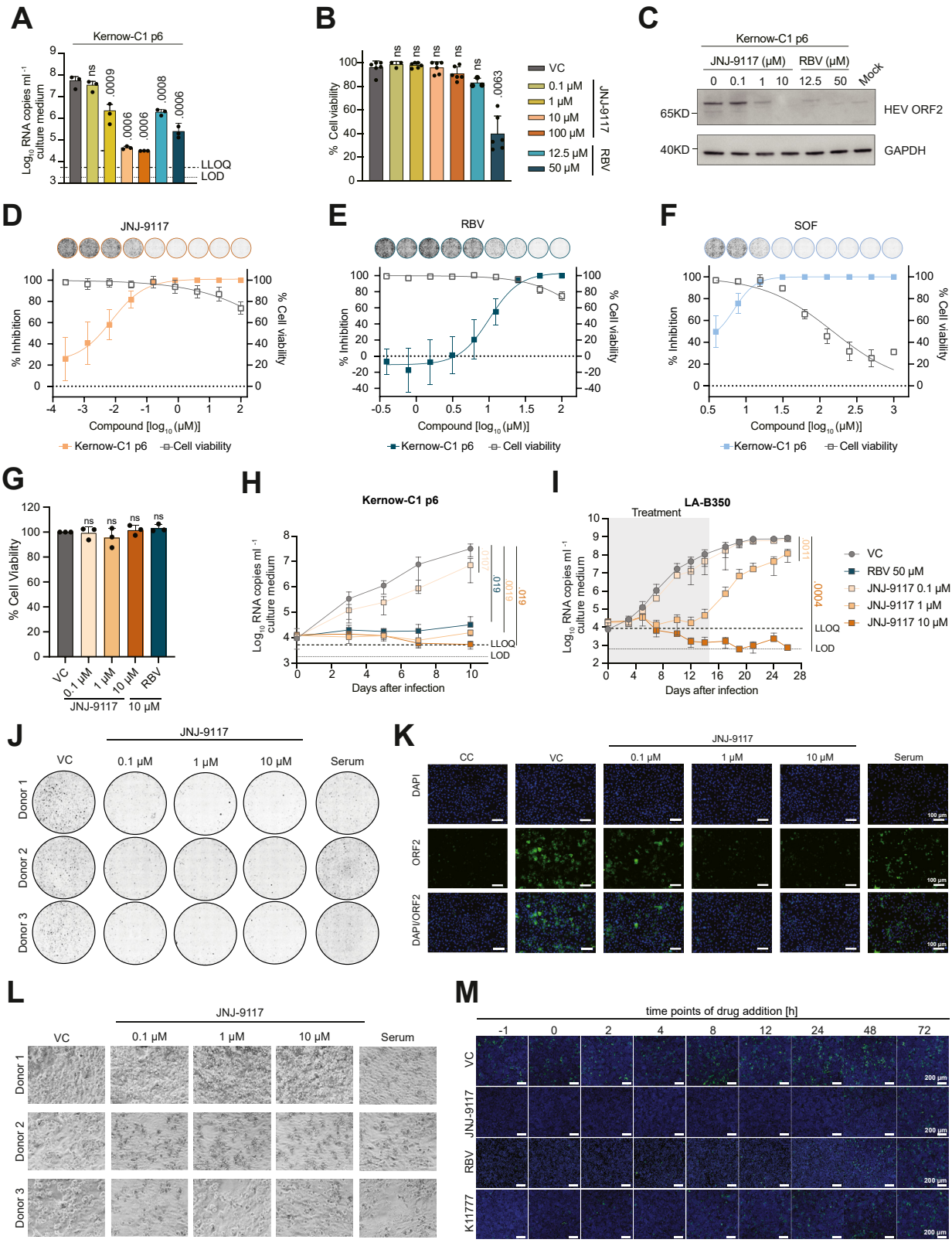
A
Kernow-C1 p6
Log10 RNA copies ml-1 culture medium
LLOQ
LOD
B
% Cell viability
VC
0.1 µM
1 µM
10 µM
100 µM
12.5 µM
50 µM
JNJ-9117
RBV
C
Kernow-C1 p6
JNJ-9117 (µM)
RBV (µM)
Mock
65KD
HEV ORF2
40KD
GAPDH
D
JNJ-9117
% Inhibition
% Cell viability
Compound [log10 (µM)]
Kernow-C1 p6
Cell viability
E
RBV
F
SOF
G
% Cell Viability
H
Kernow-C1 p6
Days after infection
I
LA-B350
Treatment
RBV 50 µM
JNJ-9117 0.1 µM
JNJ-9117 1 µM
JNJ-9117 10 µM
J
Donor 1
Donor 2
Donor 3
Serum
K
CC
DAPI
ORF2
DAPI/ORF2
100 µm
L
200 µm
M
time points of drug addition [h]
K11777

Supplementary Figure 2. In vitro assessment of antiviral activity of JNJ-9117. (*A–C*) Impact of JNJ-9117 on full genome HEV-3 Kernow-C1 p6 viral replication. HepG2/C3A cells were transfected with HEV-3 capped RNA and treated with JNJ-9117 (at 0.1, 1, 10, or 100 μmol/L) or ribavirin (RBV) (at 12.5 or 50 μmol/L) for 7 days. The supernatant was collected on day 7 after infection for quantification of viral RNA copies by (*A*) reverse-transcription quantitative polymerase chain reaction (RT-qPCR), and cells were collected for (*B*) counting total cell number for cell viability and (*C*) quantification of ORF2 by Western blot. Data are shown from 3 independent experiments. Statistical analysis was performed using (*A*) the one-way analysis of variance (ANOVA) with Dunnett's multiple comparisons test or (*B*) the Kruskal-Wallis test. In vitro antiviral activity of (*D*) JNJ-9117, (*E*) RBV, and (*F*) sofosbuvir (SOF) in HepG2/C3A cells against HEV-3 Kernow-C1 p6 virus infection. Representative whole-well images depict ORF2 capsid protein (*black dots*) on day 4 after infection. (*G*) Effect of JNJ-9117 on cell viability in HepG2/C3A cells, measured by MTT (3-(4,5-dimethylthiazol-2-yl)-2,5-diphenyltetrazoliumbromide). (*H*) Replication kinetics of HEV-3 in HepG2/C3A cells under treatment with different concentrations of JNJ-9117 (at 0.1, 1, or 10 μmol/L; *orange squares*), RBV (*blue squares*), or virus control (VC, *grey dots*) at various times after infection. (*I*) Effect of JNJ-9117 at 0.1, 1, or 10 μmol/L on the replication of rat HEV LA-B350 at different days after infection in Huh7 cells. Infected cells were incubated until day 26 after infection, with or without the compounds (*grey dots* and *orange squares*, respectively). At day 14 after infection, JNJ-9117 treatment was terminated. Viral RNA levels were quantified by RT-qPCR. (*J* and *K*) Antiviral effect of JNJ-9117 against Kernow-C1 p6–infected primary human hepatocytes (PHHs). Infected PHHs were treated with dimethyl sulfoxide (virus control, VC), anti-HEV IgG serum, JNJ-9117 (at 0.1, 1, or 10 μmol/L), or nontreated (cell control, CC). (*J*) Whole-well representation depicts stained ORF2 capsid proteins. (*K*) Representative fluorescence images show ORF2 expression in PHHs treated with JNJ-9117. ORF2, *green*; 4′,6-diamidino-2-phenylindole (DAPI), *blue*. *Scale bar* = 100 μm. (*L*) Representative bright-field images of treated PHHs. (*M*) Representative fluorescence images show ORF2 expression in Kernow-C1 p6 infected HepG2/C3A cells during the time of drug-addition assay with JNJ-9117, RBV, K11777 and VC (DMSO). ORF2, *green*; DAPI, *blue*. Data in *H* and *I* are from 3 independent biological replicates. One-way ANOVA with Dunnett's multiple comparisons test was used for the statistical analysis. Data with *error bars* represent mean ± standard deviation or mean + standard deviation. LOD, limit of detection; ns, not significant.

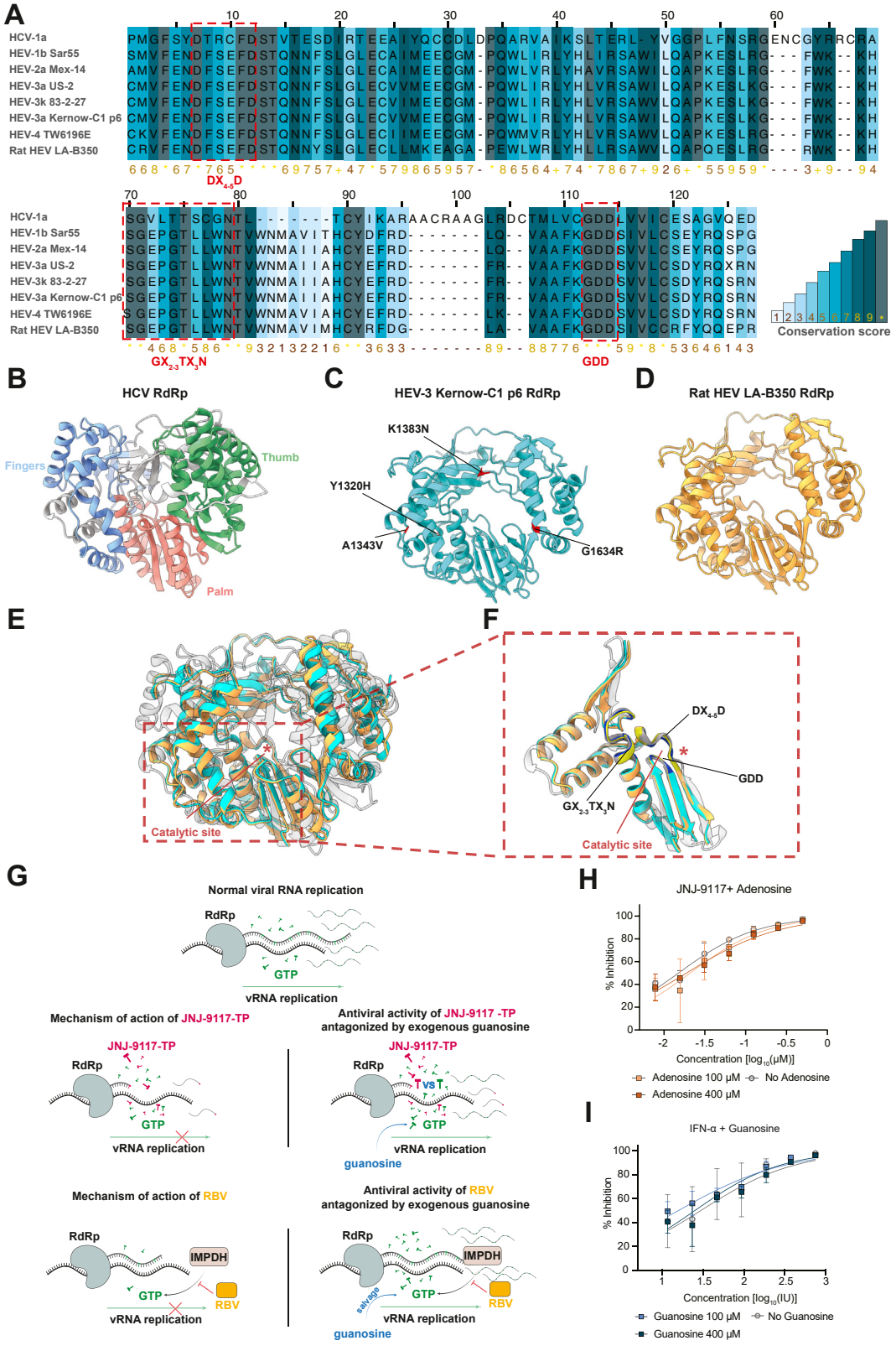
A
HCV-1a
HEV-1b Sar55
HEV-2a Mex-14
HEV-3a US-2
HEV-3k 83-2-27
HEV-3a Kernow-C1 p6
HEV-4 TW6196E
Rat HEV LA-B350
DX4-5D
GX2-3TX3N
GDD
Conservation score
B
HCV RdRp
Fingers
Thumb
Palm
C
HEV-3 Kernow-C1 p6 RdRp
K1383N
Y1320H
A1343V
G1634R
D
Rat HEV LA-B350 RdRp
E
Catalytic site
F
DX4-5D
GDD
GX2-3TX3N
Catalytic site
G
Normal viral RNA replication
RdRp
GTP
vRNA replication
Mechanism of action of JNJ-9117-TP
JNJ-9117-TP
Antiviral activity of JNJ-9117 -TP antagonized by exogenous guanosine
T vs T
guanosine
Mechanism of action of RBV
IMPDH
RBV
Antiviral activity of RBV antagonized by exogenous guanosine
salvage
H
JNJ-9117+ Adenosine
% Inhibition
Concentration [log10(μM)]
Adenosine 100 μM
No Adenosine
Adenosine 400 μM
I
IFN-α + Guanosine
Concentration [log10(IU)]
Guanosine 100 μM
No Guanosine
Guanosine 400 μM

Supplementary Figure 3. Mode of action of JNJ-9117. (*A*) Amino acid sequence alignment of the HEV RdRp catalytic site domain from a broad range of HEV strains with that of HCV-1a. Highly conserved crucial motifs at catalytic sites within the polymerase core are indicated by *dashed red boxes*. (*B*) Richardson diagram shows the overall architecture of HCV RdRp with the typical right hand shape (Protein Data Bank: 1C2P). The following color code has been used to distinguish its structural domains: *blue* – fingers; *green* – thumb; *red* – palm. (*C*) Schematic representation of the HEV-3 RdRp (Kernow-C1 p6) predicated by ColabFold. Predicated locations of ribavirin (RBV)-associated (Y1320H, K1383N, and G1634R) and sofosbuvir (SOF)-associated (A1343V) mutations are marked in *red*. (*D*) The 3-dimensional model of the rat HEV (LA-B350) RdRp generated by ColabFold. (*E*) Structural alignment of the HCV (*grey*), HEV-3 (*cyan*), and rat HEV (*gold*) RdRp (same orientation as *B*, *C*, and *D*). For clarity, the C-tail of HCV RdRp was removed. An *asterisk* marks the catalytic site. (*F*) Zoomed figure of the marked box in *E*, with the same color codes as in *E*. Three motifs have been marked to show the conservation between them, with motifs related to HCV, HEV-3, and rat HEV marked in respectively *dark grey*, *cobalt*, and *yellow*. The shown domains (residue 214 to 332 in HCV, residue 1454 to 1565 in HEV-3, and residue 1408 to 1513 in rat HEV) align with a root mean square deviation of $\sim$1 Å (75 aligned α-carbon atoms for HCV and HEV-3, and 68 aligned α-carbon atoms for HCV and rat HEV) for both structural alignments. ChimeraX was used for alignment and making the Figure panels. (*G*) Schematic representation of the proposed mechanism of action of JNJ-9117 and the known effect of RBV on HEV replication. IMPDH, inosine 5′-monophosphate dehydrogenase; vRNA, viral RNA. (*H*) The dose-response curves of JNJ-9117 (0.5–0.0078 μmol/L) against HEV-3 Kernow-C1 p6/luc under adenosine treatment (at 0, 100, or 400 μmol/L). (*I*) Combination treatment with IFN-α and guanosine (100 or 400 μmol/L). Data in *H* and *I* represent mean $\pm$ standard deviation from 2 independent biological replicates.

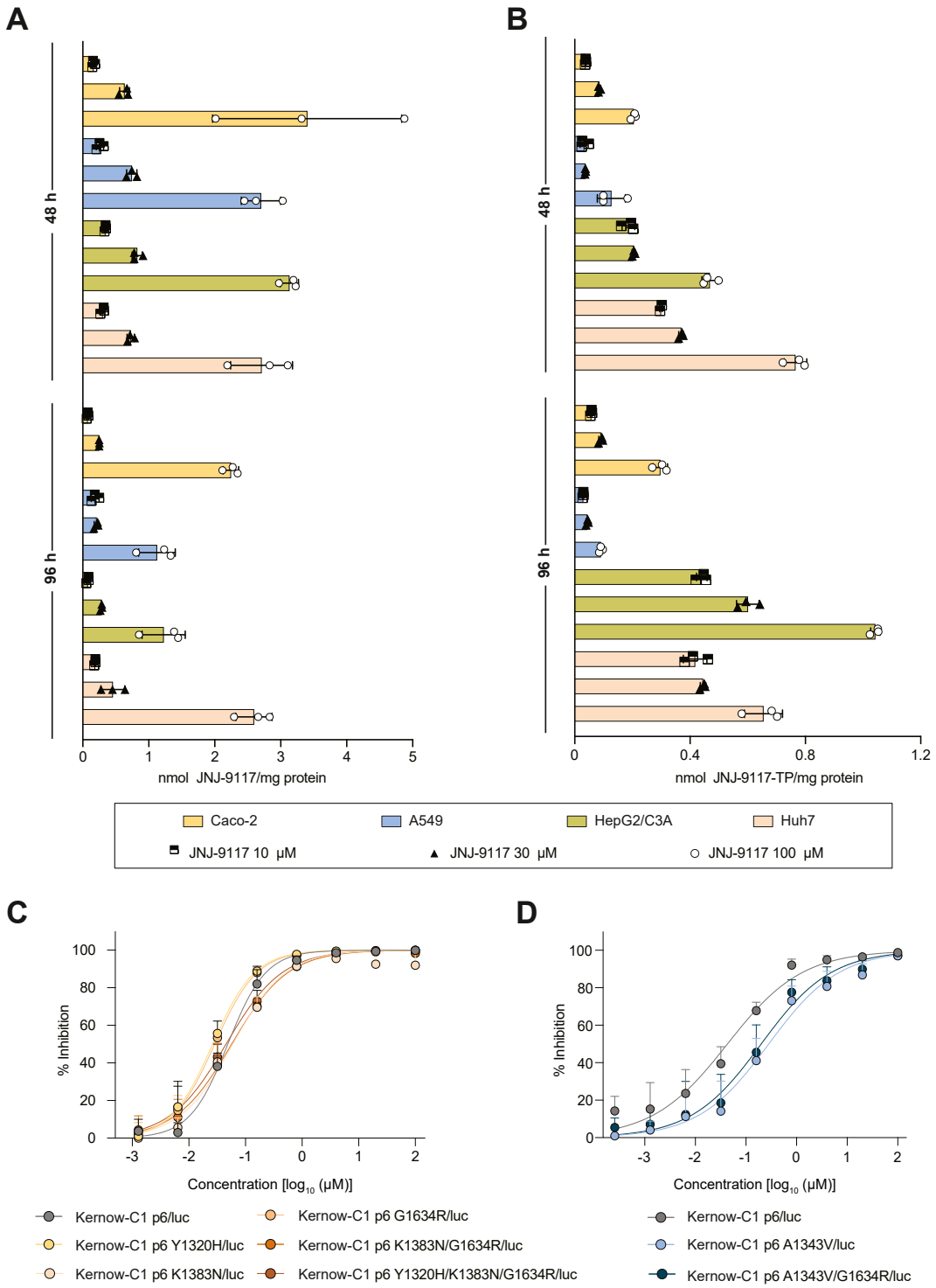

Supplementary Figure 4. The metabolism of JNJ-9117 and its sensitivity to different mutant variants of HEV-3 in vitro. (*A* and *B*) Concentrations of JNJ-9117 (prodrug) and its active metabolite JNJ-9117-TP were measured in Caco-2, A549, HepG2/C3A, and Huh7 cells at 48 hours or 96 hours after electroporation without HEV RNA, after which cells were exposed to JNJ-9117 (10, 30, or 100 μmol/L). Data are mean $\pm$ standard deviation of 3 samples from 1 independent biological experiment. (*C* and *D*) Dose-response curves of different ribavirin- or sofosbuvir-associated HEV-3 Kernow-C1 p6 mutant variants under treatment of JNJ-9117 (1.3/0.256 nmol/L to 100 μmol/L) in Huh7 or HepG2 cells. Data are mean + standard deviation from 3 independent biological replicates.

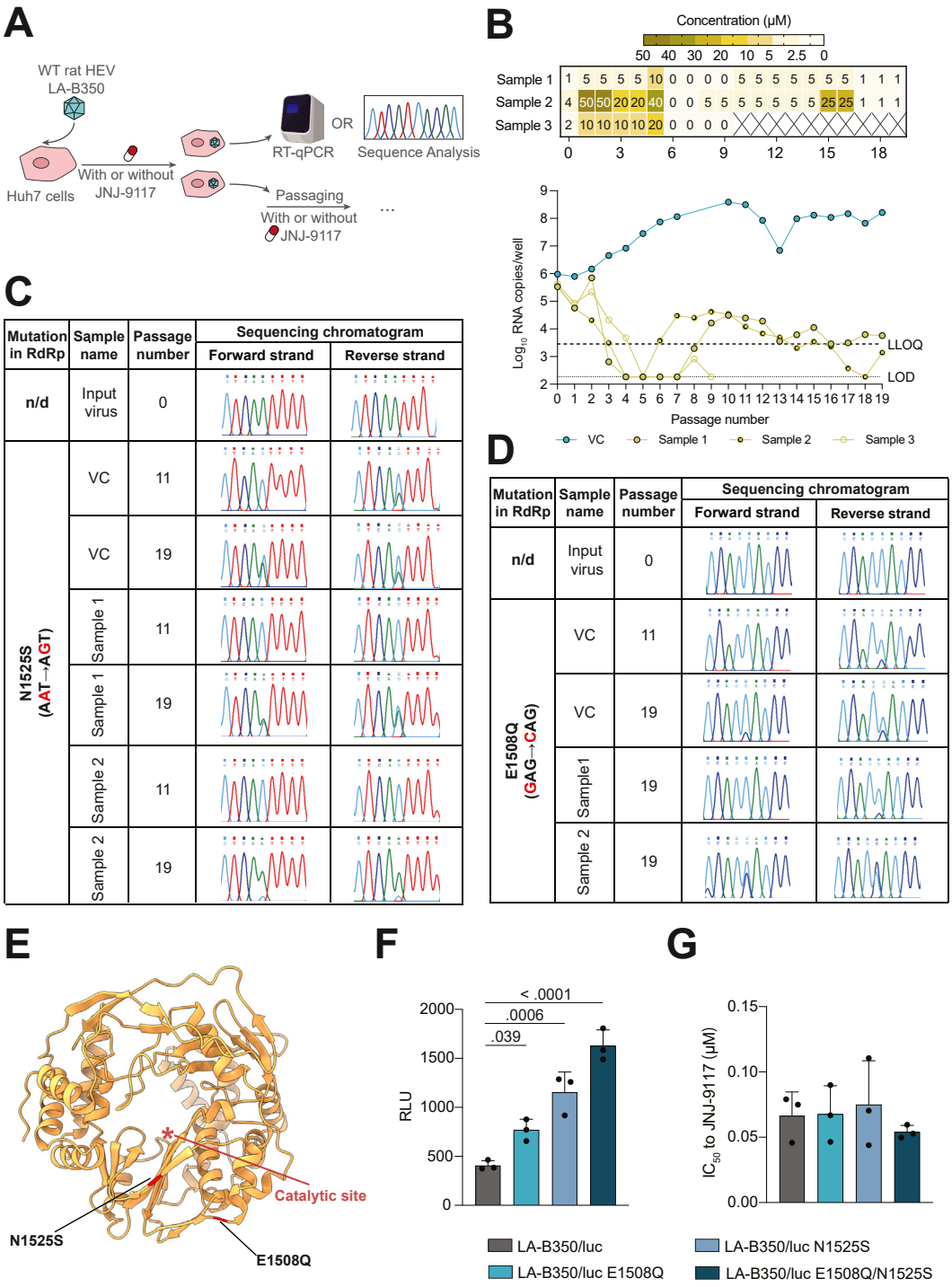

Supplementary Figure 5. Selection of JNJ-9117-resistant rat HEV variants in vitro. (*A*) Schematic overview of the protocol used to select for JNJ-9117-resistant rat HEV variants. Rat HEV-infected cells were exposed to suboptimal concentrations of JNJ-9117 for 19 passages (12 weeks in total, with 1 passage lasting 3 to 4 days). RT-qPCR, reverse-transcription quantitative polymerase chain reaction; WT, wild-type. (*B*) Intracellular HEV RNA levels in the JNJ-9117–treated and virus control (VC) wells were quantified at each passage via RT-qPCR. Sequencing chromatograms (from both the forward and reverse strand) highlight the (*C*) N1525S and (*D*) E1508Q mutation in the RdRp domain within the WT (input virus), virus control samples (VC), and JNJ-9117-selected samples (sample 1 and 2) at passage 11 and 19. n/d, not detected. (*E*) The mutations N1525S and E1508Q were mapped onto a ColabFold-predicted protein structure of the rat HEV RdRp, with their positions highlighted in *red*. (*F*) Effect of mutations (E1508Q, N1525S, or E1508Q/N1525S) on the replication of luciferase-based rat HEV replicons in Huh7 cells. RLU, relative light units. (*G*) IC_{50} of JNJ-9117 against the different mutated rat HEV replicons or the WT equivalent. Data with *error bars* represent mean + standard deviation from 3 independent biological replicates. One-way analysis of variance with Dunnett's multiple comparisons test in *F* and *G* for the statistical analysis.

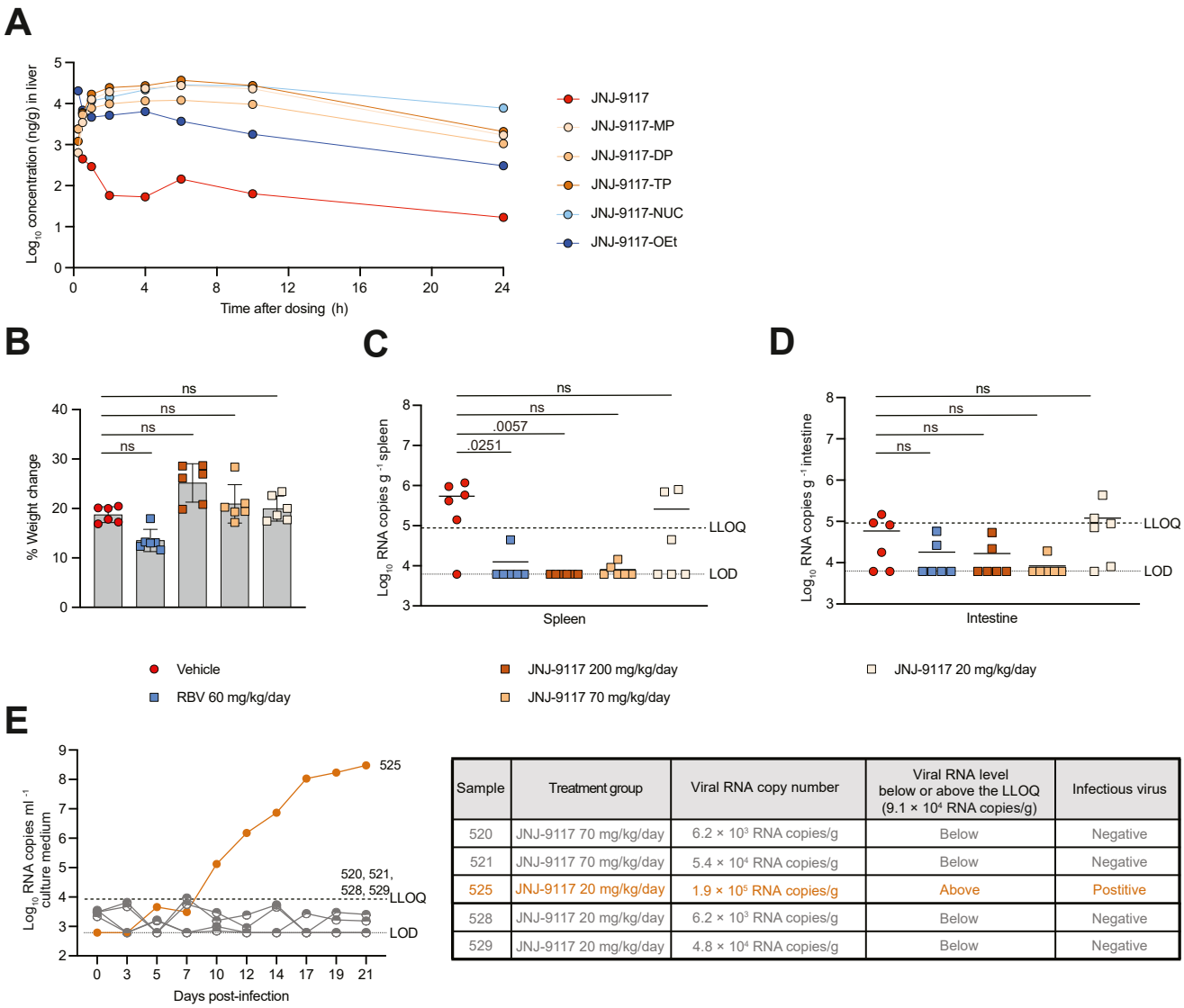

Sample	Treatment group	Viral RNA copy number	Viral RNA level below or above the LLOQ (9.1×10^4 RNA copies/g)	Infectious virus
520	JNJ-9117 70 mg/kg/day	6.2×10^3 RNA copies/g	Below	Negative
521	JNJ-9117 70 mg/kg/day	5.4×10^4 RNA copies/g	Below	Negative
525	JNJ-9117 20 mg/kg/day	1.9×10^5 RNA copies/g	Above	Postitive
528	JNJ-9117 20 mg/kg/day	6.2×10^3 RNA copies/g	Below	Negative
529	JNJ-9117 20 mg/kg/day	4.8×10^4 RNA copies/g	Below	Negative

Supplementary Figure 6. Pharmacokinetics and in vivo efficacy of JNJ-9117 in a prophylactic setting. (*A*) Liver pharmacokinetics of JNJ-9117 after a single oral dose of JNJ-9117 (200 mg/kg) administered to athymic nude rats. (*B*) Percentage of weight change measured for the individual rats (*dots* and *squares*) on day 12 after infection compared with the weight on day 0 after infection. ns, not significant. (*C* and *D*) Viral RNA levels in the spleen and the intestine of infected rats on day 12 after infection. Rats were treated with vehicle or compound (ribavirin [RBV] or JNJ-9117 at 3 different doses) and infected with rat HEV LA-B350. Treatment of the vehicle and JNJ-9117 groups started 12 hours before infection and continued twice daily, whereas treatment of the RBV group started 2 hours before infection and continued once daily. (*E*) Presence of infectious content in liver samples from JNJ-9117–treated rats. *Left panel*: Viral replication kinetics in Huh7 cells infected with rat HEV isolated from various liver samples. *Right panel*: Viral RNA levels in the tested liver samples. Statistical analysis was performed using the Kruskal-Wallis test. LOD, limit of detection.

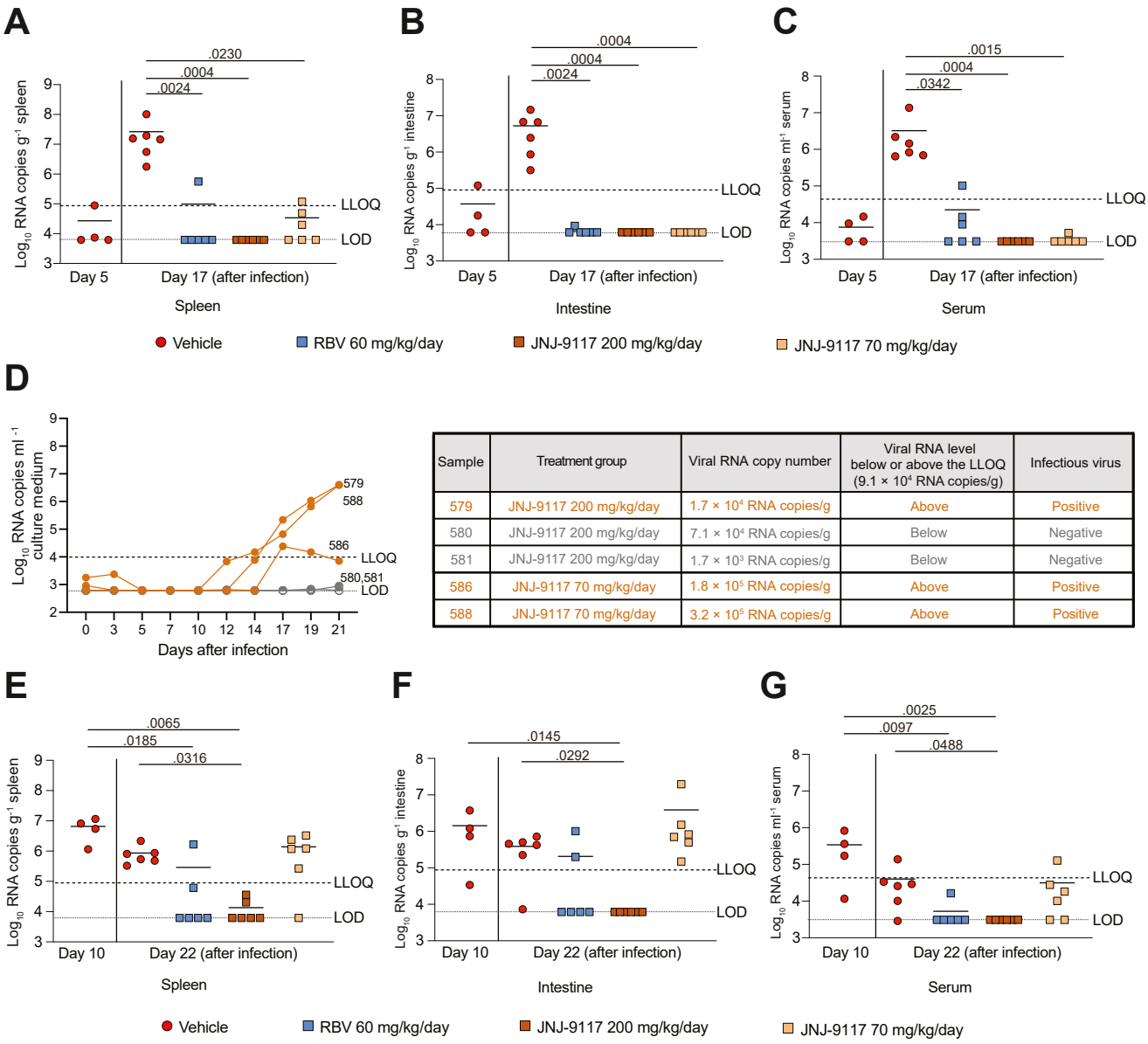

Sample	Treatment group	Viral RNA copy number	Viral RNA level below or above the LLOQ (9.1×10^4 RNA copies/g)	Infectious virus
579	JNJ-9117 200 mg/kg/day	1.7×10^4 RNA copies/g	Above	Positive
580	JNJ-9117 200 mg/kg/day	7.1×10^4 RNA copies/g	Below	Negative
581	JNJ-9117 200 mg/kg/day	1.7×10^3 RNA copies/g	Below	Negative
586	JNJ-9117 70 mg/kg/day	1.8×10^5 RNA copies/g	Above	Positive
588	JNJ-9117 70 mg/kg/day	3.2×10^5 RNA copies/g	Above	Positive

Supplementary Figure 7. In vivo efficacy of JNJ-9117 in a therapeutic setting. Viral RNA levels in the spleen, intestine, and serum of rat HEV-infected rats on (*A–C*) days 5 and 17 after infection or (*E–G*) days 10 and 22 after infection. Infected rats were treated with vehicle, ribavirin (RBV) (60 mg/kg/d), or JNJ-9117 at 2 different doses. Rats were treated from (*A–C*) days 5 to 16 or (*E–G*) days 10 to 21 after infection. Statistical analysis was performed using the Kruskal-Wallis test. LOD, limit of detection. (*D*) Presence of infectious content in liver samples of JNJ-9117–treated rats from the in vivo therapeutic experiment with start of treatment on day 5 after infection. *Left panel*: Kinetics of viral replication in Huh7 cells of rat HEV present in the different liver samples. *Right panel*: Viral RNA levels in the tested liver samples.

Mutation	Rat 1			Rat 2			Rat 3		
	day 0 pt	day 49 pt	day 70 pt	day 0 pt	day 49 pt	day 70 pt	day 0 pt	day 49 pt	day 70 pt
P134A (CCG→GCG)	n/d	n/d	n/d	n/d	n/d	n/d			
E305G (GAG→GGG)							n/d	n/d	n/d
F555S (TTC→TCC)				n/d	n/d	n/d	n/d	n/d	n/d
V558A (GTG→GCG)	n/d	n/d	n/d	n/d	n/d	n/d			
P605L (CCT→CTT)							n/d	n/d	n/d
N1525S (AAT→AGT)	n/d	n/d		n/d			n/d	n/d	

Non-dominant mutation

Dominant mutation

n/d: not detected

day 0 pt = day 60 after infection

Supplementary Figure 8. ORF1 sequencing results from fecal samples of rats during the selection of JNJ-9117–resistant rat HEV in vivo. Sanger sequencing results of the entire ORF1 region of rat HEV in fecal samples of the 3 rats on days 0, 49, and 70 posttreatment (pt).

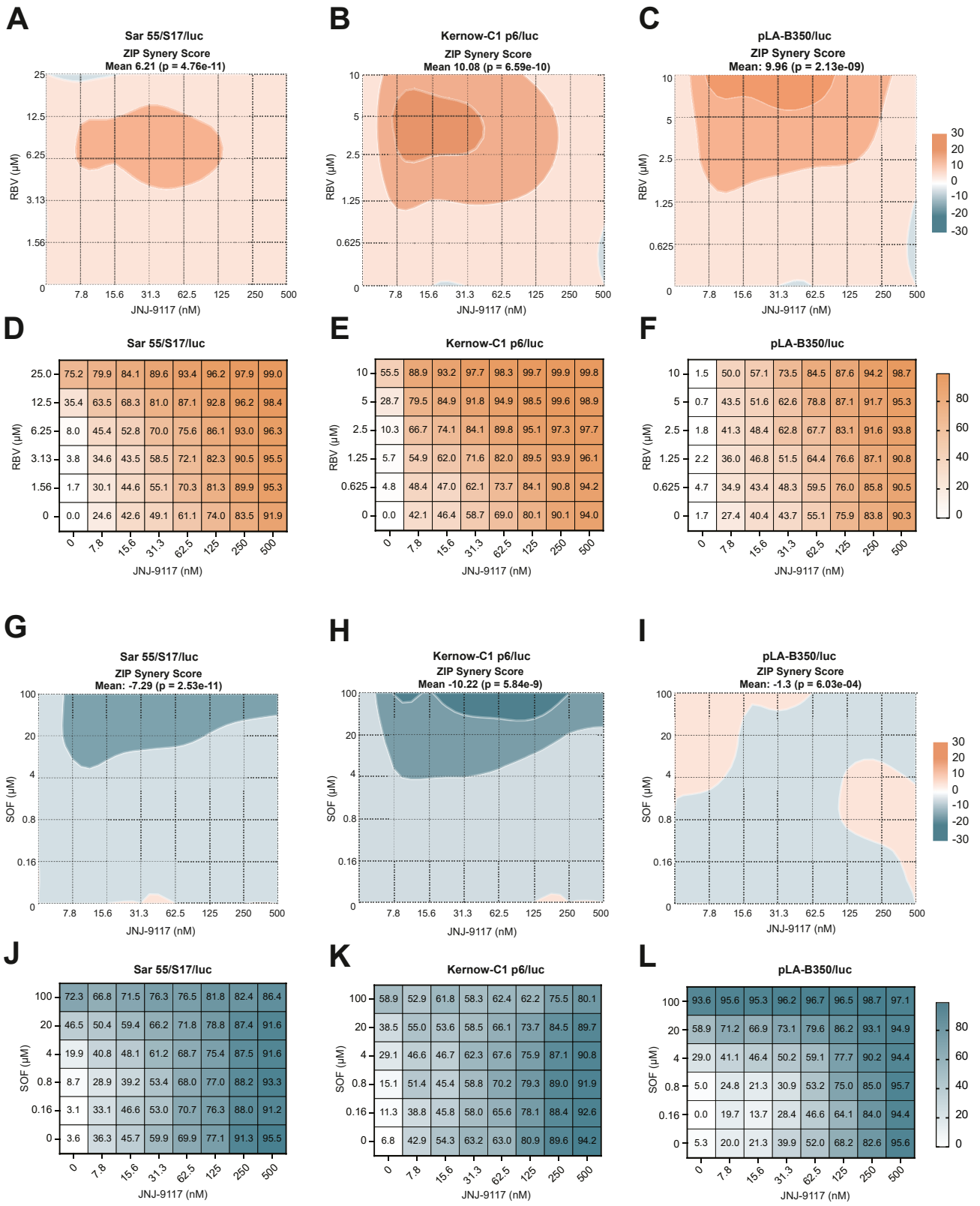

Supplementary Figure 9. In vitro effect of antiviral combinations on HEV replication in Huh7 cells. The topographic 2-dimensional map of synergy scores for the combination JNJ-9117 with (*A–C*) ribavirin (RBV) or (*G–I*) sofosbuvir (SOF) on viral replication of different HEV variants (HEV-1 Sar55/S17/luc, HEV-3 Kernow-C1 p6/luc, and rat HEV pLA-B350/luc). Synergy scores were based on ZIP analysis determined in SynergyFinder. The ZIP score stands for the response beyond expectation in percentage. In the range of ZIP −10 to <10, the compounds are likely to act in an additive manner, whereas a score of 10 or more indicates synergism and less than −10 indicates antagonism. The dose-response matrix for the combination (*D–F*) RBV/JNJ-9117 or (*J–L*) SOF/JNJ-9117, depicted as percentage inhibition of viral replication in Huh7 cells. The combination graphics represent the means of 3 independent experiments.

Supplementary Table 1. Antiviral Activity of Compounds From the Janssen Pharmaceutica Proprietary Library Against the Hepatitis E Virus 3 (Kernow-C1 p6/luc) and Rat Hepatitis E Virus (pLA-B350/luc) Subgenomic Replicons in Huh7 Cells

	HEV-3 Kernow-C1 p6/luc		Rat HEV pLA-B350/luc	
Compound ID	IC_{50} (μmol/L)	CC_{50} (μmol/L)	IC_{50} (μmol/L)	CC_{50} (μmol/L)
44901794	>50	>50	4.52	>50
44901668	0.063	>50	0.009	>50
44464791	0.25	>50	0.11	>50
44449090	0.035	104.80	0.00028	64.61
44901801	0.64	>50	0.038	>50
44901682	2.16	>50	7.19	>50
44901689	4.04	>50	5.57	>50
JNJ-9117	0.057	>50	0.036	>50
44901703	0.10	>50	0.046	>50
44901710	1.26	>50	0.85	>50
44901717	0.11	>50	0.0041	>50
44449783	0.13	>50	0.023	>50
44449790	0.058	>50	0.0099	>50
39232795	50.28	>50	27.44	>50
39499677	0.025	5.16	0.000011	3.36
39622198	87.03	>50	82.24	>50
44678459	12.92	>50	6.01	>50
44899505	3.06	>50	7.90	>50
45067834	>50	>50	0.50	>50

CC_{50}, 50% cytotoxic concentration.

Supplementary Table 2. Detailed Information of Primary Human Hepatocyte Donors

Lot No.	CHM2221-HE-C	NHM2251-HE-N	CHM2225-HE-Z
Species	Human	Human	Human
Sex	Male	Male	Male
Race/ethnicity	Caucasian	Hispanic	Caucasian
Age	51	47	73
Body mass index	24.3 kg/m^2	25.8 kg/m^2	28.0 kg/m^2
Smoke	Yes	N/A	No
Alcohol use	No	N/A	No
Drug use	No	N/A	No
Pathology	Cholangiocarcinoma	Head trauma/intracerebral hemorrhage	Hepatocellular carcinoma
Seeding density	2.4×10^5 cells/cm^2	1.6×10^5 cells/cm^2	2.1×10^5 cells/cm^2

N/A, not available.